Specific *Arabidopsis* HSP90.2 alleles recapitulate RAR1 cochaperone function in plant NB-LRR disease resistance protein regulation

David A. Hubert[a,1,2], Yijian He[a,1], Brian C. McNulty[a,3], Pablo Tornero[a,4], and Jeffery L. Dangl[a,b,c,d,5]

Departments of [a]Biology and [c]Microbiology and Immunology, [b]Curriculum in Genetics and Molecular Biology, and [d]Carolina Center for Genome Sciences, University of North Carolina, Chapel Hill, NC 27599

This contribution is part of the special series of Inaugural Articles by members of the National Academy of Sciences elected in 2007.

Contributed by Jeffery L. Dangl, May 3, 2009 (sent for review April 10, 2009)

Both plants and animals require the activity of proteins containing nucleotide binding (NB) domain and leucine-rich repeat (LRR) domains for proper immune system function. NB-LRR proteins in plants (NLR proteins in animals) also require conserved regulation via the proteins SGT1 and cytosolic HSP90. RAR1, a protein specifically required for plant innate immunity, interacts with SGT1 and HSP90 to maintain proper NB-LRR protein steady-state levels. Here, we present the identification and characterization of specific mutations in *Arabidopsis* HSP90.2 that suppress all known phenotypes of *rar1*. These mutations are unique with respect to the many mutant alleles of HSP90 identified in all systems in that they can bypass the requirement for a cochaperone and result in the recovery of client protein accumulation and function. Additionally, these mutations separate HSP90 ATP hydrolysis from HSP90 function in client protein folding and/or accumulation. By recapitulating the activity of RAR1, these novel hsp90 alleles allow us to propose that RAR1 regulates the physical open–close cycling of a known ''lid structure'' that is used as a dynamic regulatory HSP90 mechanism. Thus, in *rar1*, lid cycling is locked into a conformation favoring NB-LRR client degradation, likely via SGT1 and the proteasome.

innate immunity | *Pseudomonas syringae* | SGT1 | STAND ATPase protein

Plants have evolved a highly complex immune system centered on pathogen recognition via the evolutionarily-conserved NB-LRR proteins. Pathogen-triggered activation of NB-LRR proteins leads to several responses, including cell wall strengthening, transcriptional reprogramming, and a form of programmed cell death termed the hypersensitive response (HR). Because their function often results in cell death, proper maintenance of NB-LRR protein levels and activation state are vital to the health of the plant (1).

NB-LRR proteins can be divided into 2 structural subgroups based on the presence of either a likely coiled-coil (CC) or Toll interleukin-1 receptor (TIR) domain at their N termini. Either of these N-terminal domains is followed in both subgroups by a middle nucleotide binding (NB) site and a C-terminal leucine-rich repeat (LRR). This general structure is not only conserved across all plants but extends to NOD/Caterpiller/NLR proteins that mediate various processes in mammalian innate immunity (2).

Just as the domain composition of these intracellular receptors is conserved from plants to animals, so is the regulation of their steady-state accumulation. Cytosolic HSP90 and the cochaperone SGT1 have been previously demonstrated to not only be important for regulation of NB-LRR proteins in plants, but also in regulation of NLR function in animals (3). A third protein called RAR1 appears to play a role in innate immunity specifically in plants (4).

All 3 of these proteins can independently interact with one another; the CS domain of SGT1b, or the CHORDI domain of RAR1, can interact with the N-terminal ATPase domain of HSP90; the CHORDII domain of RAR1 also interacts with the CS domain of SGT1 (5). The interaction of SGT1 with HSP90 has been shown to be required for SGT1 function (6). Mutation of SGT1 can suppress *rar1* for some NB-LRR functions, but not all (7). However, the relationship between RAR1 and HSP90 is less understood.

We present and characterize specific missense alleles of HSP90.2 in the reference plant, *Arabidopsis*, that suppress *rar1*. These *hsp90.2* alleles are uniquely interesting in that they can bypass the requirement for a cochaperone and result in recovery of client protein accumulation and function.

We used genetic and biochemical analyses to demonstrate that these hsp90.2 mutant proteins act on NB-LRR proteins affected by *rar1*, suppressing all identified *rar1* phenotypes. We further show that these mutations are functionally distinct from previously-identified *hsp90.2* mutations (8), including a null allele. These specific missense changes in hsp90.2 enable a separation of HSP90 ATP hydrolysis activity and HSP90 function in client protein accumulation. By recapitulating the activity of RAR1 in its absence, the phenotypes of these *hsp90.2* mutants strongly suggest that RAR1 physically enhances the transition state of HSP90 as it moves from a ''lid open'' ADP-bound conformation to a ''lid closed'' ATP-bound conformation.

Results

Identification of Alleles of RAR1 and HSP90. To identify new genes required for RPM1 function in *Arabidopsis*, we performed 2 genetic screens. Both took advantage of sensitized genetic backgrounds. The first was a modification of a previous screen (9), using a β-estradiol-inducible copy of the *avrRpm1* bacterial type III effector gene whose product is recognized in *Arabidopsis* by the RPM1 NB-LRR protein (Fig. S1*A*). Given the very high recovery ratio of *rpm1* alleles compared with second-site loci isolated previously (9), we modified the screen by crossing into this background a well-characterized transgenic, myc-epitope tagged copy of *RPM1* expressed from the native promoter (Fig. S1*A* and ref. 10). Approximately 1 million M_2 plants were

Author contributions: D.A.H., Y.H., P.T., and J.L.D. designed research; D.A.H., Y.H., B.C.M., and P.T. performed research; D.A.H., B.C.M., and P.T. contributed new reagents/analytic tools; D.A.H., Y.H., and J.L.D. analyzed data; and D.A.H., Y.H., and J.L.D. wrote the paper.

The authors declare no conflict of interest.

Freely available online through the PNAS open access option.

[1]D.A.H. and Y.H. contributed equally to this work.

[2]Present address: BASF Plant Sciences LLC, Research Triangle Park, NC 27709.

[3]Present address: Athenix Corp., Research Triangle Park, NC 27709.

[4]Present address: Instituto de Biología Molecular y Celular de Plantas, Universidad Politecnica de Valencia, Camino de Vera s/n, 46022 Valencia, Spain.

[5]To whom correspondence should be addressed. E-mail: dangl@email.unc.edu.

This article contains supporting information online at www.pnas.org/cgi/content/full/0904877106/DCSupplemental.

screened from 200 ethyl methanesulfonate (EMS)-mutagenized seed lots. Putative surviving mutants were then assayed for loss of disease resistance in response to pathogen-delivered AvrRpm1 to eliminate mutations in the estradiol-inducible system (see *Materials and Methods*).

Various candidate genes previously implicated in RPM1 function were then sequenced in the remaining putative mutants. They included the endogenous copy of *RPM1*, the transgenic copy of *RPM1-myc*, *RAR1*, and all 4 genes encoding *Arabidopsis* cytosolic HSP90 (8–11). Four mutations in *RAR1* and 1 allele of *HSP90.2* were found, *hsp90.2–6* (Fig. S2). The *rar1* alleles are consistent with previous mutations: premature stops, splicing defects, and disruption of zinc-coordinating residues (12, 13). The allele of *hsp90.2* displayed intermediate susceptibility and full penetrance, as previously found for *hsp90.2–1* and *hsp90.2–3* (8). Mutations were not found in these loci in the remaining mutants.

The second screen was a *rar1* suppressor screen, aimed at identifying loci that would restore the loss of NB-LRR protein accumulation, and the consequent loss of NB-LRR function, that are the principal *rar1* phenotypes (13). Approximately 200,000 EMS-mutagenized M_2 individuals from 50 M_1 seed lots of *rar1–21* were spray-inoculated with *Pto* DC3000(*avrPphB*) (see *Materials and Methods*). This strain is recognized in *Arabidopsis* by the RPS5 NB-LRR protein (14). We used RPS5 as the read-out in this screen because *rar1* exhibits a strong and uniform disease susceptibility phenotype to *Pto* DC3000(*avrPphB*). We reasoned that a suppressor would be obviously disease resistant against this susceptible background.

We identified 5 independent second-site mutants defining 3 loci in this screen. Although *hsp90.2* has previously been shown to have no effect on RPS5 (8), 2 of the mutants are missense mutations in the *hsp90.2* gene based on map-based cloning and subsequent sequencing of both mutant alleles (Fig. S2*B*). The other 2 loci will be discussed elsewhere. To avoid confusion, we will henceforth refer to *hsp90.2* alleles that lose RPM1 function by the original notation, *lra* (loss of recognition of *avrRpm1*) (13), and alleles that suppress *rar1* as *rsp* (*rar1 s*uppressor). Like all of the *lra* alleles, *hsp90.2–7^{rsp}* is completely recessive. However, based on disease symptoms after bacterial inoculation, *hsp90.2–8^{rsp}* behaves as a weak semidominant allele (see *Materials and Methods*).

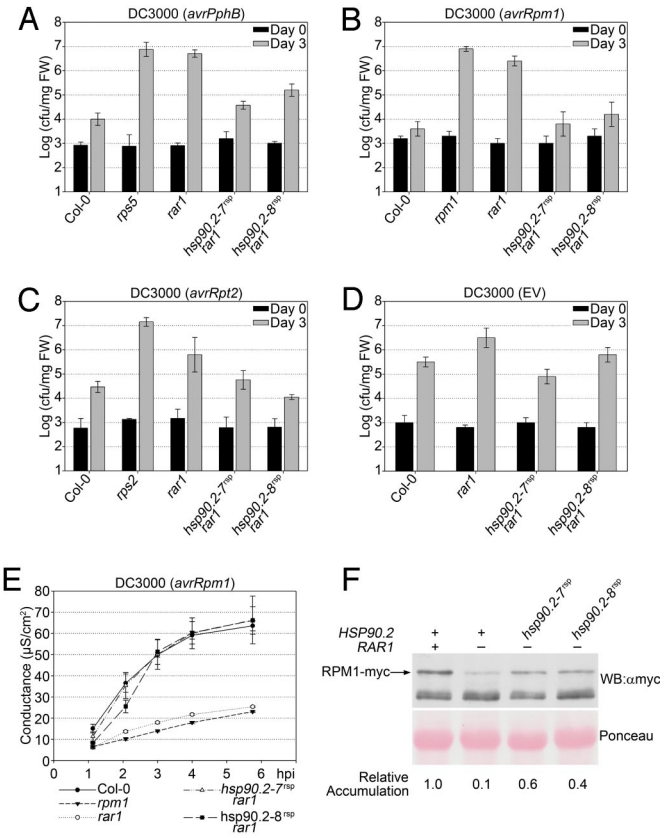

Fig. 1. *rsp* alleles suppress all known *rar1* phenotypes. (*A–D*) Bacterial growth assays comparing *rar1* mutants to *hsp90.2^{rsp} rar1* double mutants. Note the logarithmic scale. *hsp90.2^{rsp}* mutants suppress *rar1* phenotypes for disease resistance mediated by *RPS5* (*A*), *RPM1* (*B*), and *RPS2* (*C*). (*D*) *hsp90.2^{rsp}* mutants suppress the *rar1* phenotype of decreased basal resistance to *Pto* DC3000 (7). (*E*) *hsp90.2^{rsp}* alleles suppress the *rar1* phenotype of loss of *RPM1*-mediated HR. An increase in conductivity is indicative of the release of ions from cells undergoing HR. (*F*) *hsp90.2^{rsp}* alleles suppress the *rar1* phenotype of lowered steady-state accumulation of RPM1-myc protein.

***hsp90.2^{rsp}* Alleles Suppress all Known *rar1* Phenotypes.** Inexplicably, *hsp90.2^{lra}* alleles were previously shown to specifically impact RPM1 function, and not the function of other tested NB-LRR proteins (8). Conversely, *rar1* affects the steady-state accumulation of all tested NB-LRR proteins, and the function of many, by lowering their accumulation below a functional threshold (7, 15). Hence, we did not expect to identify *hsp90.2* alleles in our RPS5-based *rar1* suppressor screen. We determined whether the *rsp* alleles suppressed *rar1* phenotypes of other NB-LRR-dependent disease resistance specificities. The *hsp90.2^{rsp}* alleles variably suppressed *rar1* with respect to RPS5 function (Fig. 1*A*), RPM1 function (Fig. 1*B*), and RPS2 function (Fig. 1*C*).

rar1 mutants express decreased basal disease resistance to the virulent pathogen *Pto* DC3000 (7). The only molecular phenotype ever ascribed to *rar1* is diminution of steady-state NB-LRR protein accumulation as noted above. Thus, this phenotype suggests an as-yet-undocumented role for RAR1 on NB-LRR proteins that might either function in basal defense and/or weak recognition of the type III effectors delivered by *Pto* DC3000 (16). Notably, both *hsp90.2^{rsp}* alleles also suppress this phenotype (Fig. 1*D*).

We used the release of ions into solution by inoculated plant leaf discs to measure the ability of *hsp90.2^{rsp}* to suppress the loss of HR associated with *rar1* (17). Although neither *rpm1* nor *rar1* are able to generate an HR upon delivery of AvrRpm1, *rar1 hsp90.2^{rsp}* double mutants display the same level of HR as wild-type Col-0 plants (Fig. 1*E*). The suppression of this particular *rar1* phenotype is in marked contrast to results obtained with *sgt1b* as a *rar1* suppressor (7).

We next assayed whether the *hsp90.2^{rsp}* alleles were able to suppress the most direct *rar1* mutant phenotype, a decrease in NB-LRR protein accumulation (13). We introgressed a transgenic RPM1-myc-epitope-tagged derivative driven from its native promoter (10) into each *hsp90.2^{rsp} rar1* mutant. In these double mutants, the *hsp90.2^{rsp}* alleles suppressed the very low RPM1 accumulation observed in *rar1* (Fig. 1*F*). Hence, the *hsp90.2^{rsp}* alleles suppress the key biochemical phenotype of *rar1*, at least with respect to RPM1 and probably more generally, given the pathology data presented in Fig. 1.

Because RPM1, RPS2, and RPS5 are CC-NB-LRR proteins, we addressed whether a *RAR1*-dependent, TIR-NB-LRR protein is also suppressed by the *hsp90.2^{rsp}* alleles. RPP4 conditions disease resistance to the oomycete pathogen, *Hyaloperonospora arabidopsidis* (*Hpa*) (18). In this case, the HR is likely to be required for disease resistance, whereas it is likely to be dispensable for resistance to bacterial pathogens. We noted that both *hsp90.2^{rsp} rar1* lines expressed higher RPP4 function than *rar1* (Fig. S3*A*) and exhibited higher levels of HR (Fig. S3*B*). Hence, the *hsp90.2^{rsp}* alleles also suppress *rar1* for a TIR-NB-LRR and in a context where HR is likely to be the key mechanism of disease resistance.

The possibility existed that the recovery of disease resistance

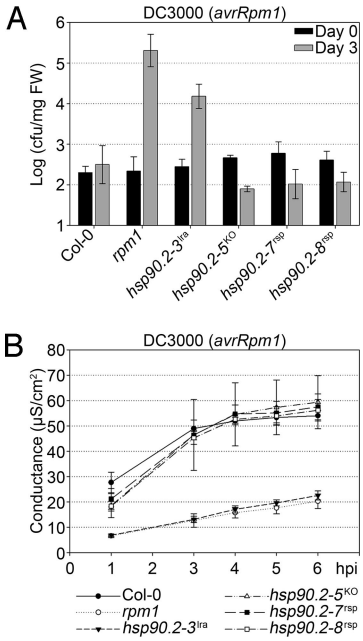

Fig. 2. *hsp90.2*^{rsp} mutants are phenotypically distinct from an *hsp90.2*^{lra} single mutant and an *hsp90.2* T-DNA insertion null mutant. *hsp90.2*^{rsp}, *hsp90.2*^{lra}, and *hsp90.2*^{KO} single mutant plants are compared with each other and Col-0 and *rpm1* plants. (*A*) Bacterial growth assay for recognition of *Pto* DC3000(*avrRpm1*) by RPM1. (*B*) Conductivity assay measuring the HR triggered by RPM1 activation after recognition of AvrRpm1.

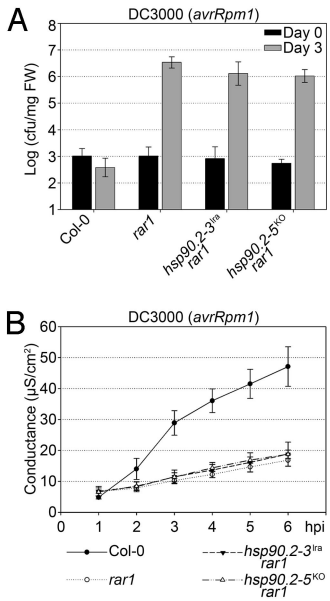

Fig. 3. Neither an *hsp90.2*^{lra} allele nor the *hsp90.2*^{KO} null allele suppress *rar1*. (*A*) Bacterial growth assay measuring disease resistance to *Pto* DC3000 (*avrRpm1*) mediated by RPM1. Wild-type Col-0 and *rar1* mutant plants are compared with *hsp90.2–3*^{lra} *rar1* and *hsp90.2*^{KO} *rar1* double mutants. (*B*) Conductivity assay measuring the HR to *Pto* DC3000 (*avrRpm1*).

observed in *hsp90.2*^{rsp} *rar1* double mutants is not specific, but rather a result of general metabolic perturbation resulting in disease resistance. Such perturbations are typically accompanied by an increase in the levels of defense marker proteins such as PR-1 (19). However, we did not observe an obvious increase in PR-1 levels in *hsp90.2*^{rsp} lines.

We previously demonstrated that a presumed truncated protein product made by the *rar1–21* allele used as the parent in this screen, which would express only CHORD-I, is, surprisingly, able to coimmunoprecipitate HSP90. This coimmunoprecipitation was not observed with the *rar1–20* null allele or the W47stop allele, *rar1–28* (ref. 8 and Y. Belkhadir, personal communication). We constructed *rar1–28 hsp90.2*^{rsp} combinations for both *rsp* alleles. We assayed for RPM1 function to rule out the possibility of a *rar1* allele-specific effect. We clearly observed suppression of the *rar1* phenotype in *rar1–28 hsp90.2*^{rsp} double mutants; hence the effect of the *rsp* alleles on RPM1 function is not *rar1–21* allele specific.

***hsp90.2*^{rsp} Alleles Have No Phenotype in RAR1.** We isolated the *hsp90.2*^{rsp} single mutants by backcrossing and assayed them for RPM1 function. As seen in Fig. 2*A*, the *hsp90.2*^{rsp} single mutants express wild-type RPM1 function. Hence, the *hsp90.2*^{rsp} single mutants are phenotypically distinct from the *hsp90.2*^{lra} alleles (8), which all express partial loss of RPM1-mediated disease resistance. We also monitored HR in the *hsp90.2*^{rsp} single mutants. *hsp90.2*^{rsp} alleles again expressed wild-type phenotypes (Fig. 2*B*).

The HSP90.2^{rsp} proteins might counterbalance the decrease in NB-LRR protein accumulation observed in *rar1* by conditioning "hyperaccumulation" above wild-type levels. We thus introgressed RPM1-myc into each *hsp90.2*^{rsp} mutant and assayed for RPM1-myc protein accumulation. We detected wild-type RPM1-myc protein levels in the single mutant lines. We conclude that there is no increased NB-LRR protein activity indicative of "hyperchaperoning" by the *hsp90.2*^{rsp} alleles. Thus, these alleles are true suppressors of the loss of *RAR1* molecular activity and are not merely overcoming the *rar1* phenotype by increased overall expression of client protein.

***hsp90.2*^{lra} and *hsp90.2*^{KO} Alleles Do Not Suppress *rar1*.** We next tested whether either *hsp90.2*^{KO} or a reference *hsp90.2–3*^{lra} allele (encoding D80N, a mutation analogous to the well-studied yeast D79N; ref. 20) could suppress *rar1* for RPM1 function. We constructed the appropriate double mutants and noted that both were as susceptible to *Pto* DC3000(*avrRpm1*) as *rar1* (Fig. 3*A*). Conductivity measurements of RPM1-mediated HR in these double mutants (Fig. 3*B*) gave similar results, supporting the conclusion that neither *hsp90.2*^{KO} nor an *hsp90.2–3*^{lra} allele can suppress *rar1*. Thus, the *hsp90.2*^{rsp} alleles are also phenotypically distinct from both a null allele (Fig. 3) and the classic ATPase dead *hsp90.2–3*^{lra} (Figs. 2 and 3).

***hsp90.2*^{rsp} Alleles Are Not Null Alleles.** Although both *hsp90.2*^{rsp} alleles encode missense changes, there remained a possibility that they are functionally null. If so, then 1 of the 3 remaining cytosolic HSP90 proteins might compensate for the loss of HSP90.2 in these alleles, as previously noted for *hsp90.2*^{KO} (8). *Arabidopsis* has 4 genes encoding cytosolic HSP90, 3 of which, including *HSP90.2*, reside in a cluster. The fourth, *HSP90.1*, lies ≈1.3 Mbp away on the same chromosome. We wanted to establish whether stepwise elimination of HSP90 function would reveal null phenotypes, which we could then compare with *hsp90.2–3*^{lra} and *hsp90.2–7*^{rsp} alleles. We were unable to recover *hsp90.2–5*^{KO} *hsp90.1*^{KO} double mutants. However, we did identify plants homozygous for *hsp90.1*^{KO} and heterozygous for *hsp90.2–5*^{KO}. These were stunted and expressed high accumulation of anthocyanins, loss of apical dominance, and very low fecundity. Selfed progeny segregated lethals. Hence, *HSP90.1* is synthetically lethal with *HSP90.2*, suggesting that the overall level of cytosolic HSP90 has a minimum threshold for viability. Importantly, we were able to obtain *hsp90.2–3*^{lra} *hsp90.1*^{KO}, *hsp90.2–7*^{rsp} *hsp90.1*^{KO}, and *hsp90.2–8*^{rsp} *hsp90.1*^{KO} double mutants. These were viable and as healthy as either single mutant.

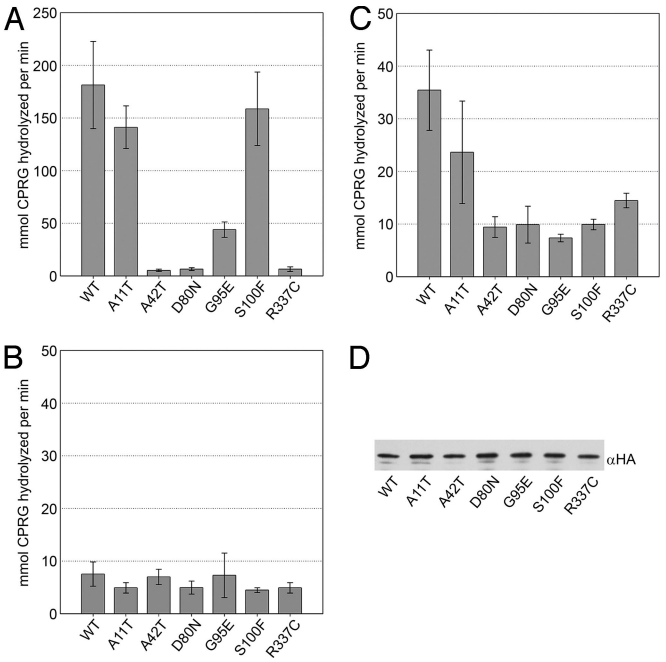

Fig. 4. Interactions between hsp90.2 mutant proteins and RAR1 or SGT1b does not correlate with phenotype. (*A–C*) β-Galactosidase assay quantification of the results of yeast 2-hybrid interaction measurements between HSP90.2 and mutant variants with RAR1 (*A*), SGT1a (*B*), or SGT1b (*C*). (*D*) HSP90.2 and mutant variants accumulate to equivalent levels in yeast as measured by Western blot. RAR1 interacts normally with SGT1a in this assay.

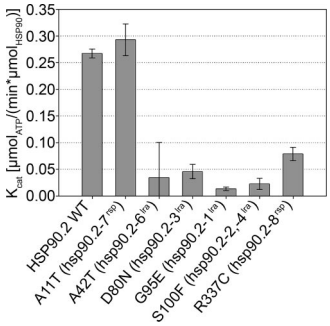

Fig. 5. HSP90 ATPase activity does not predict *hsp90.2* mutant phenotype. In vitro ATPase activity of HSP90.2 and mutant variants with a range of ATP concentrations was used to determine the K_{cat}. HSP90 concentration was 5 μM, and ATP concentrations ranged between 0 and 1.2 mM (see *Materials and Methods*).

Hence, *hsp90.2–3*^{lra}, *hsp90.2–7*^{rsp}, and *hsp90.2–8*^{rsp} maintained the HSP90 activity required to support proper growth and development in the absence of HSP90.1.

We thus conclude that none of the tested *rsp* or *lra* alleles are null for HSP90 activity. Our collected genetic data strongly suggest that the *hsp90.2*^{rsp} alleles are active, and that they recapitulate the molecular activity of RAR1 on client NB-LRR accumulation.

Analysis of Interactions Between hsp90.2 Mutant Proteins with RAR1 and SGT1. Given the correlation between the region of HSP90 mutated in both of our genetic screens and the region of HSP90 that physically interacts with RAR1 and SGT1 (see Introduction), we were interested in finding out whether our HSP90 mutants were affected in their ability to interact with RAR1 and SGT1 in the yeast 2-hybrid system. As shown in Fig. 4, wild-type HSP90.2 can interact with both RAR1 and SGT1b, but not SGT1a, which is consistent with previously-published coimmunoprecipitation experiments (8). Hence, this system is likely to accurately reflect in vivo interactions in *Arabidopsis*.

We found that all 4 of the hsp90.2^{lra} proteins lost interaction with SGT1b in yeast 2-hybrid (Fig. 4*C*). Three lost interaction with RAR1 (Fig. 4*A*). The exception was S100F (hsp90.2–2^{lra}), previously noted (8) to be partially penetrant, which maintained a strong interaction with RAR1. The 2 rsp mutant proteins exhibited opposing RAR1 and SGT1b interactions. The A11T (hsp90.2–7^{rsp}) protein maintained strong interactions with both RAR1 and SGT1b. However, the R337C (hsp90.2–8^{rsp}) protein lost the ability to interact with both RAR1 and SGT1b. None interacted with SGT1a (Fig. 4*B*), indicating that this protein is likely to be irrelevant to HSP90.2 function. Western blot analysis showed that all mutant proteins were expressed equally well in yeast (Fig. 4*D*). The loss of interaction between R337C (hsp90.2–8^{rsp}) and both RAR1 and SGT1b suggests that these interactions are not necessary for restoration of NB-LRR function in this allele. This result is consistent with restoration of several different RAR1-dependent NB-LRR functions in *rar1 sgtb* double mutants (7).

We were unable to observe an interaction between HSP90.2 and any tested fragment of RPM1 by yeast 2-hybrid analysis. However, we did see a strong interaction between GST-HSP90 fusion purified from *Escherichia coli* and an HA epitope-tagged version of RPM1 produced via in vitro transcription and translation in wheat germ lysates (21). Using this system, we did not observe any difference in the ability of lra or rsp mutant HSP90.2 proteins to interact with RPM1. Hence, it is unlikely that an overall change in NB-LRR protein interaction with HSP90 causes the various *hsp90.2* mutant phenotypes.

ATPase Activity Is Not Predictive of HSP90 Activity in NB-LRR Function. All *hsp90.2* missense alleles obtained from our 2 screens were either located in the ATPase domain itself or in the case of R337C^{rsp} in a part of the middle domain physically adjacent to the ATPase domain in the HSP90 crystal structure (Fig. S4). Thus, differences in ATPase activity associated with the N-terminal HSP90 domain (22) might also explain the different properties of the mutant HSP90.2 proteins. We purified recombinant wild-type HSP90.2 and all of the lra and rsp variants (see *Materials and Methods*). Circular dichroism analyses of the purified proteins showed that all variants had an equivalent proportion of α-helix and β-sheet indicative of proper folding. The ability of these proteins to hydrolyze ATP was measured in an ATP-regenerating system (see *Materials and Methods*).

Nearly all of the hsp90.2–8^{lra} alleles are missense changes in amino acids that contact bound nucleotide in the crystal structure, and D80N (hsp90.2–3^{lra}; D79N in *Sc*HSP90) loses ATP hydrolysis. Hence, it was unsurprising that these proteins lacked ATPase activity (Fig. 5). R337C (hsp90.2–8^{rsp}) expressed only very weak ATPase activity (≈2-fold above negative control). Surprisingly, A11T (hsp90.2–7^{rsp}), maintained full ATPase activity, but with a ≈5-fold increase in the observed K_M [wild type = 0.04 μM ± 0.01; A11T (hsp90.2–7^{rsp}) = 0.20 μM ± 0.05]. However, plant cytosolic ATP concentrations were ≈3 mM (23), suggesting that the change in K_M is probably not relevant to the phenotype exhibited by the mutant. Addition of RAR1 and/or SGT1b to these assays did not alter ATPase activity; this negative result may merely mean that we lack other required conditions and/or components for in vitro reconstruction.

N-Terminal Dimerization Is Retained in hsp90.2^{rsp} Proteins. Yeast HSP90 functions as a dimer formed via separate N-terminal and C-terminal dimerization domains. In yeast, N-terminal dimerization is mediated by a short-N-terminal stretch of each monomer (Fig. S4) and requires ATP binding (24). Using the same

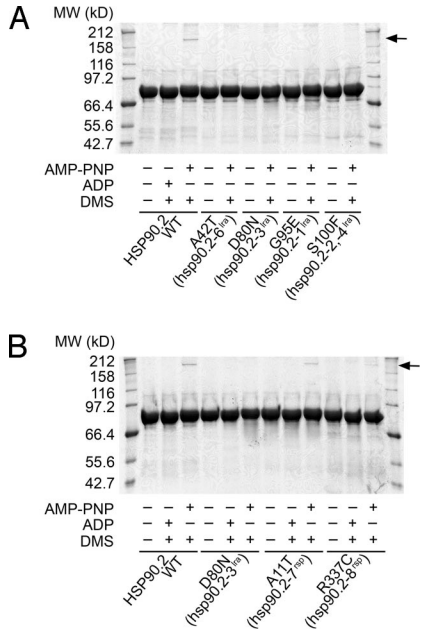

Fig. 6. HSP90.2^{rsp} mutant proteins retain dimerization capability. Chemical cross-linking of wild-type and mutant forms of HSP90.2 in the presence of ADP or the nonhydrolysable ATP analog AMP-PNP. All variants of HSP90.2 are unable to dimerize in the presence of ADP. However, although no lra mutant variants (*A*) are able to dimerize even in the presence of AMP-PNP, both rsp mutant variants (*B*) can dimerize in the presence of AMP-PNP. The experiment was performed with an HSP90 concentration of 0.25 mg/mL, 15 molar equivalents of DMS, and 10 mM nucleotide.

assay, we found that dimerization of full-length *Arabidopsis* HSP90.2 depended on the presence of the nonhydrolyzable ATP analogue, adenosine 5′-[β,γ-imido]triphosphate (AMP-PNP). We did not observe HSP90.2 dimers in the absence of AMP-PNP or the presence of ADP. We also tested purified lra and rsp HSP90 mutant proteins for dimerization. The lra mutant variants were unable to dimerize in the presence of any tested nucleotide (Fig. 6*A*) The rsp mutant variants could dimerize, A11T (hsp90.2–7^{rsp}) more than R337C (hsp90.2–8^{rsp}), but both less than wild type (Fig. 6*B*). Addition of RAR1 and/or SGT1b to these assays did not alter dimerization activity under these conditions. Hence, ATP binding is required for *Arabidopsis* HSP90 dimerization.

The proportion of HSP90.2 that we observed in the dimerized form was low compared with the results reported for yeast HSP90 (24). It is unclear whether this was caused by our buffer conditions or it is an intrinsic property of *Arabidopsis* HSP90.2. However, this lower proportion of dimer was not caused by our cross-linking conditions, because increasing the concentration of cross linker ≈10-fold did not result in an increased proportion of dimerized HSP90.2.

In yeast, an ATP-independent C-terminal domain is sufficient (defined using N-terminal truncations), but not necessary (defined using C-terminal truncations), for HSP90 dimerization (25). Given our dimerization results and the positions of the rsp mutations on HSP90.2, we wanted to make sure that we were assaying the ATP dependent N-terminal activity in our assay. We purified HSP90.2 containing a short C-terminal truncation, known to abolish ATP-independent dimerization in yeast HSP90 (see *Materials and Methods* and ref. 24). This protein was unable to dimerize, even in the presence of AMP-PNP (Fig. S5). We thus conclude that the C-terminal dimerization domain of *Arabidopsis* HSP90.2 is necessary, but not sufficient (e.g., as in the cases where the N-terminal domain is mutated), for dimerization of *Arabidopsis* HSP90.2 and that the dimerization we measured was caused by the N-terminal domain.

Discussion

We performed 2 genetic screens to identify components affecting RPM1-mediated disease resistance in *Arabidopsis*. We demonstrate here that 2 specific *hsp90.2* mutations suppress *rar1* and restore NB-LRR protein accumulation, and hence, function. These *hsp90.2^{rsp}* alleles demonstrate that HSP90.2 plays a broader role in disease resistance in *Arabidopsis* than previously considered (8). The *hsp90.2^{rsp}* alleles are unique in 3 ways: (*i*) The particular mutations, A11T and R337C, have not been identified in any genetic screen, although the residues are strictly conserved across all eukaryotic species. (*ii*) These mutations translate into HSP90 proteins that bypass the requirement for a cochaperone. (*iii*) Most importantly, these mutations result in HSP90 alleles that result in a recovery of client protein accumulation and function (Table S1). The particular features of the *hsp90.2^{rsp}* alleles, together with emerging structural analyses of HSP90 and its cochaperones, allow us to examine HSP90 function and propose an explicit mechanism for the function of the RAR1 cochaperone in NB-LRR protein stabilization.

hsp90.2–7^{rsp} is recessive and encodes an A11T change. *hsp90.2–8^{rsp}* is weakly semidominant and encodes a R337C change. Both suppress all known *rar1* phenotypes to similar degrees. For example, both partially suppress *rar1* for RPS5 function and fully suppress *rar1* for RPM1 and RPS2 function, as measured by restoration of HR and pathogen growth restriction. They also suppress the *rar1*-enhanced disease susceptibility phenotype. Most importantly, both restore accumulation of RPM1-myc in *rar1*. Neither *rsp* allele has any discernible phenotype in the presence of RAR1. Neither expresses enhanced RPM1 activity in the presence of RAR1. Both provide some level of HSP90.2 function, at least as it pertains to viability in the context of a decrease in overall HSP90 levels. We used these 2 *hsp90.2^{rsp}* alleles and the 4 previously-identified *hsp90^{lra}* alleles (8) in a variety of tests designed to address how they might differentially influence 3 properties of HSP90: interaction with RAR1 and SGT1b, ATPase activity, and HSP90 dimerization. The rsp mutant proteins have different properties in these assays, as noted in *Results*, although both can dimerize to differing degrees.

The *rsp* alleles allowed us to examine the relationship between HSP90 ATPase activity and HSP90 function. It has long been assumed that ATPase activity is required for HSP90 function (26, 27). The data presented here argue against this concept in 2 ways. First, R337C (hsp90.2–8^{rsp}) restores NB-LRR accumulation in *rar1*, yet the R337C mutation exhibits a nearly full loss of ATPase activity. Further, R337C is a more efficient suppressor of *rar1* than A11T based on its semidominance, yet it nevertheless has lower ATPase activity than A11T. Hence, at least in the absence of RAR1, high ATPase activity is not required for NB-LRR accumulation. Second, D80N (hsp90.2–3^{lra}), which is unable to bind ATP, does provide some function, to the extent that the *hsp90.2–3^{lra} hsp90.1^{KO}* double mutant was viable, and expresses no novel phenotype. In fact, given the nearly lethal phenotype observed with a half-dose of HSP90.2 in the absence of HSP90.1 the D80N mutation must exhibit more than half the activity of wild-type HSP90.2. But we leave open the possibility of an entirely different explanation for the phenotype of the *lra* alleles than simple loss of activity. Together, these 2 lines of evidence suggest that HSP90 ATPase activity can be separated from HSP90 function as it pertains to the modulation of NB-LRR function.

Fig. 7 presents close-up views of part of the X-ray structure of nucleotide-bound yeast HSP90 (28). Because HSP90 is so highly conserved across kingdoms, the *Arabidopsis* sequence threads onto this sequence with high confidence. The 2 HSP90 monomers in this structure are held together via an N-terminal clasp

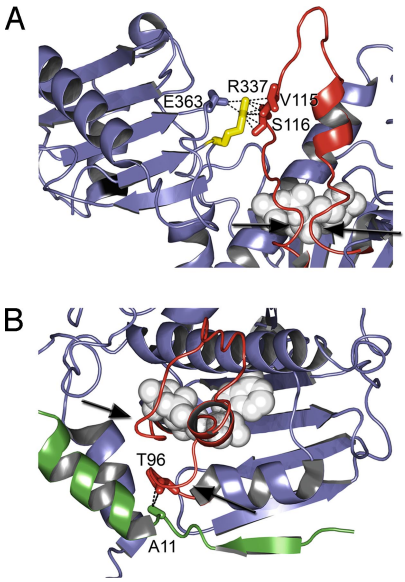

Fig. 7. *rsp* mutations affect residues in the lid region of HSP90 in the closed conformation. Ribbon structures of yeast HSP90 (Protein Data Bank ID code 2CG9) bound to ATP (light gray). This lid (red) is hinged at G95 and G122 and swings 180° to fold over the nucleotide-binding pocket (yeast G94 and G121). (*A*) R337 (yellow) coordinates interaction of the central client-binding domain (purple, left) with the flexible lid (red) by interacting with V115 and S116 in the lid region and E363 within the middle domain of HSP90 (yeast R346, V114, S115, and E372). (*B*) A11 (yeast A10) from 1 monomer (green) interacts directly with T96 (yeast T95; red side chain) within the hinge of the other monomer. Black arrows indicate the locations of the hinges of the lid.

(and at the C terminus, although that is not relevant here). Each monomer of HSP90 contains a lid segment, hinged at residues G95 and G122 (Fig. 7), that swings through nearly 180° from its open position in the ADP-bound form of HSP90, to a closed ATP-bound conformation. This movement locks in the ATP molecule and places the catalytic arginine (371 in *Arabidopsis*; 380 in yeast) in position for interaction with the γ-phosphate of ATP. This movement also facilitates formation of the N-terminal dimerization clasp (28).

The structures of nucleotide-bound HSP90 suggest a mechanism for *rar1* suppression by the rsp mutant proteins and present a clear prediction for RAR1 function in NB-LRR accumulation. We postulate that A11T and R337C act to favor the transition between the ADP- and ATP-bound conformations of HSP90.2, a transition characterized by the open–close cycling of the hinged lid. HSP90 has an 5-fold higher affinity for ADP over ATP (20). Thus, favoring the transition state, perhaps counter-intuitively, favors the ATP bound conformation. The HSP90^{rsp} proteins demonstrate that lid conformation is critical for client stabilization. Our ATP hydrolysis results suggest that ATP hydrolysis per se is irrelevant to HSP90 activity. Instead, the conformation of the N-terminal domain is important. However, it is likely that ATP hydrolysis is part of a regulatory mechanism allowing for control of the relative time spent in either conformation.

In the nucleotide-bound HSP90 structure (Fig. 7*A*), V114 and S115 from the closed lid (Fig. 7*A* in red) contact R337 from the same monomer. In R337C (hsp90.2–8^{rsp}), these interactions are very likely to be destabilized, favoring a lid-open conformation, consistent with an inability to continue efficient nucleotide cycling. As shown in Fig. 7*B*, A11T lies within the N-terminal strand of HSP90. This strand switches from an intramolecular interaction in the ADP-bound, lid-open form of HSP90 to an intermolecular interaction with the opposing subunit of the HSP90 dimer in the ATP-bound, lid-closed form (Fig. S4). This intermolecular interaction should act to maintain and/or strengthen N-terminal dimerization. A11 contacts T96 near the base of the hinge on the opposing monomer. Consequently, the A11T mutation would be expected to both decrease the binding of the N-terminal strand to the opposing monomer and alter the stability of the lid-closed conformation. This conformational effect would decrease, but not abolish N-terminal dimerization, as we observed in Fig. 6.

We propose that destabilization of the lid-closed conformation by R337C is responsible for the diminution of dimerization, loss of interaction with RAR1 (and SGT1b), and nearly full loss of ATPase activity. The loss of RAR1 interaction with this presumably misregulated "floppy lid" does not have ill effects for the function of this HSP90 allele because it is, in essence, blind to RAR1 presence or absence. Hence, the R337C mechanism of action defines normal RAR1 function, namely, enhancing the cycling of the HSP90.2 lid, N-terminal dimerization cycling and client accumulation. This proposal is consistent with A11T, where we observed interaction with RAR1 (and SGT1b), normal nucleotide hydrolysis, some dimerization, and a recessive phenotype (meaning that it is a less efficient *rar1* suppressor than the semidominant R337C). We propose that A11T is also able to bypass normal RAR1 function via its less efficient ability to maintain a lid-closed conformation.

Our model is consistent with recent observations studying the kinetics of N-terminal dimerization using a single molecule FRET-based HSP90 folding assay. In these in vitro experiments, 2 conformational states between the lid-open and lid-closed conformations were studied (29, 30). These intermediate conformations were shown to be rate-limiting steps in the ATPase reaction cycle (30). This work also demonstrated that the yeast cochaperone AHA1 is able to enhance the rate of ATP hydrolysis by bypassing an intermediate conformational state (lid closure) that follows ATP binding and precedes N-terminal dimerization, in favor of a lid-closed, ATP-bound, dimerized, prehydrolysis state. Our interpretation of the HSP90.2 rsp proteins above is consistent with this model.

Based on this model, we expect RAR1 (and by analogy our rsp alleles) to disfavor progression of the HSP90 cycle presented by Hessling et al. (30) at different points before the lid-closed, N-terminal dimerized intermediate they define as I_2. R337C dimerizes very poorly compared with wild type, is likely to act by loosening the HSP90 lid, and is the stronger of the 2 *rsp* alleles. We infer that it diminishes the ATP-bound to the lid-closed I_1 intermediate transition proposed by Hessling et al. (30). A11T dimerizes only slight less efficiently than wild type, is likely to act by disrupting N-terminal clasp formation, and expresses less than wild-type weak ATP hydrolytic efficiency. We infer that this allele is unable to transition efficiently beyond the ATP-bound, lid-closed I_2 intermediate. Given these inferences, and the fact that A11T retains interaction with RAR1 whereas R337C loses it, we suggest that RAR1 binds to HSP90.2 at, and potentially after, the I_1 conformation. Furthermore, we suggest that RAR1 acts to slow the progression of the HSP90 conformational cycle. These transition states can be reached in the absence of nucleotide (29). Hence, our data further suggest that overall HSP90 function and consequent effects on NB-LRR function are more coupled to the HSP90 conformational state than to ATP hydrolysis per se.

The sum of our data and recent single-molecule folding studies (29, 30) suggest that NB-LRR proteins are destabilized in *rar1* because the HSP90 lid-open–lid-close cycle cannot be properly regulated, consistent with a model in which the balanced activities of RAR1, SGT1, and other cochaperones acting with HSP90 determine steady-state NB-LRR protein accumulation and signaling competence (7).

Materials and Methods

Plant Lines. Transgenic *Arabidopsis* ecotype Columbia (Col-0; line a11) containing estradiol-inducible *avrRpm1* has been described (9). For the double RPM1 screen, we used line a11 plant with an additional transgenic, myc-epitope-tagged copy of *RPM1* introgressed (13). For the *rar1* suppressor screen we used the originally-isolated *rar1–21* mutant identified in line a11 (13). For pathology and double mutant analysis, we used *rar1–21*, *rar1–28*, or *hsp90.2–3^{lra}* lines with the estradiol-inducible *avrRpm1* removed by backcrossing to Col-0 and subsequent PCR-based marker-assisted breeding (8, 13). Mutant lines used (all in Col-0 unless noted) were *rpm1–3* (31), *rps2–101c* (32), *rps5–2* (14), ecotype Ws-0 as an *RPP4* mutant control (18), and *hsp90.2–5^{KO}* (8). We constructed double mutants of *hsp90.2* alleles and *rar1–21* by identifying F_2s with a recombination event placing these linked mutations in *cis*. These plants were selfed, and resultant F_3 individuals were further selected with PCR-based markers. *hsp90.1^{KO}* was produced by selecting a homozygous insertion in the SALK T-DNA insertion line 075596 [previously referred to as hsp90.1–2; ref. 5] that was identified by molecular analysis of a segregating pool. The insertion site was confirmed by sequencing of the T-DNA-specific product.

Pathogen Strains, Inoculation, and Growth Quantification. *Pto* DC3000 derivatives containing pVSP61 (empty vector), *avrPphB*, *avrRpm1* or *avrRpt2* have been described (33). Plant inoculations and bacterial growth assays were performed as described (11). Results for all bacterial growth assays represent 3 replicates with error bars representing +/− the standard deviation, a 95% confidence interval. All assays were performed independently a minimum of 3 times with similar results. High concentrations of *Pto* DC3000 (*avrRpm1*) (OD_{600} = 0.1, 5 × 10^7 cfu/mL) were syringe-infiltrated into leaves of 4- to 5-week-old plants to induce HR. Ion leakage assays were carried out as described (17).

Hyaloperonospora arabidopsidis (*Hpa*) propagation and inoculation were performed as described (34). Ten-day-old cotyledons of plants were inoculated with the asexual spores of *Hpa* isolate Emwa1. Asexual sporangiophores were counted 7 days postinoculation on at least 40 cotyledons for each genotype. Trypan blue staining for cell death and the *Hp* structures has been described (35). Pictures of trypan blue-stained leaves were taken with a light microscope (Nikon Eclipse).

Identification and Map-Based Cloning of Mutations in *HSP90.2*. The double RPM1 screen was performed as described (9). The *rar1* suppressor screen was performed by using a spray inoculation method in which 2-week old plants were sprayed with a 10 mM $MgCl_2$ suspension containing *Pto* DC3000 (*avrPphB*) at a concentration of OD_{600} = 0.05 (2.5 × 10^7 cfu/mL) with 0.02% silwet L-77, covered with a clear lid for 4 h, and assessed for chlorosis and other symptoms of bacterial infection 4–6 days later.

Standard genetic crosses and analyses of F_1 and F_2 progeny were used. From the *rar1* suppressor screen, rough mapping was preformed by crossing *rsp rar1–21* mutants and the Landsberg *erecta rar1–10* mutant (12). F_2 plants were tested for *rsp rar1–21*-like resistance responses by spray inoculation as described above. Resistant F_2 individuals were allowed to self and confirmed in the F_3 generation. DNA from the F_2 individuals was used in PCR amplification of known PCR-based molecular markers (www.arabidopsis.org) to obtain approximate mapping positions. Independent rough mapping of the 2 mutants showed linkage to the same interval. This interval was refined by using molecular markers we developed. We used 423 resistant F_2 individuals to define a 4.5-Mb interval on the bottom arm of chromosome V containing *HSP90.2* that is known as a regulator of RPM1 stability. By sequencing *HSP90.2* in the originally-isolated double mutant, a G/A transition at position 31 (nucleotide positions relative to the translation start site of the published sequence of *HSP90.2*; At5g56030) was identified in *hsp90.2–7^{rsp}*. The other mutant, *rsp2*, also contains a mutation (C1423T giving rise to R337C) in *HSP90.2*.

Yeast 2-Hybrid Analysis. HSP90.2 and mutant derivatives were cloned into pJG4–5 by using the EcoRI and XhoI restriction sites and site-directed mutagenesis via overlap extension. RAR1, SGT1a, and SGT1b were cloned into a Gateway-compatible version of pEG202, pEG202gw (gift of Hiro Kaminaka, Tottori University, Tottori, Japan; ref. 7). Interactions were analyzed in yeast strain EGY48. Normal function of the SGT1a construct was shown by testing its interaction with RAR1 in the pJG4–5gw vector. Assays were performed with a plate reader (Tecan) as described (36). Protein levels were analyzed as described (7).

Protein Blot. For detection of RPM1-myc levels in plants, we introgressed a transgene expressing RPM1-myc from the native *RPM1* promoter as described (13). Protein extraction and immunodetection from plant tissue were carried out as described (8).

Production of Recombinant Proteins. HSP90.2, mutant variants, and a 110-aa C-terminal truncation were cloned into pGEX-6p1 as described above and transformed into RIL codon plus cells (Strategene). Cells were grown in 2× yeast extract tryptone (YT) to an OD of ≈0.4 at 37 °C, and then the temperature was decreased to 22 °C for 45 min, and cells were induced for 3 h with 1 mM IPTG. Cell pellets were resuspended in buffer A [20 mM Tris (pH 8.0), 300 mM NaCl, and 1 Complete EDTA-Free" protease inhibitor tablet (Roche)]. After resuspension, cells were lysed by using an Avestin Emulsiflex-C5. The lysates were cleared by centrifugation for 45 min at 15,000 rpm in an SS-34 rotor. The cleared lysates were run on a 5-mL High Trap glutathione column (GE Healthcare) and washed with 10 column volumes of buffer A. The protein was eluted with 5 column volumes of buffer A with 20 mM glutathione. PreScission protease (50 units/mL; GE Healthcare) was then added to the sample, and the protein was cleaved overnight at 4 °C while being dialyzed into buffer B [20 mM sodium phosphate (pH 6.5), 150 mM NaCl, 2 mM DTT]. The next morning, the protein was loaded onto a HiLoad 16/10 Q Sepharose High Performance anion exchange column equilibrated in buffer B and eluted with a 150- to 600-mM linear gradient. Fractions were analyzed for purity by SDS/PAGE, and clean fractions were pooled and dialyzed into buffer C (40 mM Hepes, 150 mM KCl, and 5 mM $MgCl_2$ at pH 7.5).

Biochemical Methods. Circular dichroism experiments were performed on a Pistar-180 circular dichroism/fluorescence spectrophotometer (Applied Photophysics). Samples at ≈20 μM were placed in a 0.1-cm cuvette, and scans were taken from 195 to 260 nm with 1-nm increments and 30,000 repetitions per increment.

ATP hydrolysis assays were performed as described (27, 37). Briefly, 2.5 μM purified HSP90 was incubated with 0.4 mM phosphoenol pyruvate, 0.25 mM NADH, and 1% PK/LDH enzyme mix (Sigma). Proteins were incubated with multiple concentrations of ATP between 0 and 1.2 mM. Experiments were performed in duplicate with a control containing 0.5 mM radicicol to measure HSP90-specific activity. Experiments were performed in 200-μL reactions in a plate reader (GENios; Tecan).

Cross-linking experiments were performed as described (24). Purified HSP90 (0.25 mg/mL) was incubated for 2 h with 10 mM ADP or AMP-PNP, after which a 15 molar excess of dimethyl suberimidate dihydrochloride (DMS) was added for an additional 2-h incubation. Reactions were stopped by addition of SDS/PAGE loading buffer and loading on an 8% gel.

ACKNOWLEDGMENTS. We thank Prof. David Toft and Dr. Sara Felts (Mayo Clinic College of Medicine, Rochester, MN) for advice and protein samples to optimize the ATPase assays; Prof. John Sondek (University of North Carolina) for use of equipment and helpful discussions; Ryan Chao, Jonny Chen, Anna Newton, Allison Osborne, David Rybnicek, and Linda Yang for help with plant maintenance and molecular genotyping; and all current and former members of J.L.D.'s laboratory. T-DNA insertion lines were provided by Joe Ecker (Salk Institute, La Jolla, CA) via the Arabidopsis Biological Resource Center. Terry Law and Petra Epple, for helpful discussions and technical advice. This work was supported by National Science Foundation *Arabidopsis* 2010 Project Grant IOB-0520003 (to J.L.D.).

1. Jones JD, Dangl JL (2006) The plant immune system. *Nature* 444:323–329.
2. Ting JP, Willingham SB, Bergstralh DT (2008) NLRs at the intersection of cell death and immunity. *Nat Rev Immunol* 8:372–379.
3. Ye Z, Ting JP (2008) NLR, the nucleotide-binding domain leucine-rich repeat containing gene family. *Curr Opin Immunol* 20:3–9.
4. da Silva Correia J, Miranda Y, Leonard N, Ulevitch R (2007) SGT1 is essential for Nod1 activation. *Proc Natl Acad Sci USA* 104:6764–6769.
5. Takahashi A, Casais C, Ichimura K, Shirasu K (2003) HSP90 interacts with RAR1 and SGT1 and is essential for RPS2-mediated disease resistance in *Arabidopsis*. *Proc Natl Acad Sci USA* 100:11777–11782.
6. Boter M, et al. (2007) Structural and functional analysis of SGT1 reveals that its interaction with HSP90 is required for the accumulation of Rx, an R protein involved in plant immunity. *Plant Cell* 19:3791–3804.
7. Holt, BF III, Belkhadir Y, Dangl JL (2005) Antagonistic control of disease resistance protein stability in the plant immune system. *Science* 309:929–932.
8. Hubert DA, et al. (2003) Cytosolic HSP90 associates with and modulates the *Arabidopsis* RPM1 disease resistance protein. *EMBO J* 22:5679–5689.
9. Tornero P, Chao R, Luthin W, Goff S, Dangl JL (2002) Large-scale structure–function analysis of the *Arabidopsis RPM1* disease resistance protein. *Plant Cell* 14:435–450.
10. Boyes DC, Nam J, Dangl JL (1998) The *Arabidopsis thaliana RPM1* disease resistance gene product is a peripheral plasma membrane protein that is degraded coincident with the hypersensitive response. *Proc Natl Acad Sci USA* 95:15849–15854.
11. Tornero P, Dangl JL (2001) A high-throughput method for quantifying growth of phytopathogenic bacteria in *Arabidopsis thaliana. Plant J* 28:475–481.
12. Muskett PR, et al. (2002) *Arabidopsis* RAR1 exerts rate-limiting control of R gene-mediated defenses against multiple pathogens. *Plant Cell* 14:979–992.

13. Tornero P, et al. (2002) *RAR1* and *NDR1* contribute quantitatively to disease resistance in *Arabidopsis* and their relative contributions are dependent on the *R* gene assayed. *Plant Cell* 14:1005–1015.
14. Warren RF, Henk A, Mowery P, Holub E, Innes RW (1998) A mutation within the leucine-rich repeat domain of the *Arabidopsis* disease resistance gene *RPS5* partially suppresses multiple bacterial and downy mildew resistance genes. *Plant Cell* 10:1439–1452.
15. Bieri S, et al. (2004) RAR1 positively controls steady-state levels of barley MLA resistance proteins and enables sufficient MLA6 accumulation for effective resistance. *Plant Cell* 16:3480–3495.
16. Chang JH, et al. (2005) A high-throughput, near-saturating screen for type III effector genes from *Pseudomonas syringae*. *Proc Natl Acad Sci USA* 102:2549–2554.
17. Torres MA, Dangl JL, Jones JD (2002) *Arabidopsis* gp91phox homologues AtrbohD and AtrbohF are required for accumulation of reactive oxygen intermediates in the plant defense response. *Proc Natl Acad Sci USA* 99:517–522.
18. van der Biezen EA, Freddie CT, Kahn K, Parker JE, Jones JDG (2002) *Arabidopsis RPP4* is a member the *RPP5* multigene family of TIR-NB-LRR genes and confers downy mildew resistance through multiple signaling components. *Plant J* 29:439–451.
19. Belkhadir Y, Nimchuk Z, Hubert DA, Mackey D, Dangl JL (2004) *Arabidopsis* RIN4 negatively regulates disease resistance mediated by RPS2 and RPM1 downstream or independent of the NDR1 signal modulator and is not required for the virulence functions of bacterial type III effectors AvrRpt2 or AvrRpm1. *Plant Cell* 16:2822–2835.
20. Prodromou C, et al. (1997) Identification and structural characterization of the ATP/ADP-binding site in the Hsp90 molecular chaperone. *Cell* 90:65–75.
21. Kawasaki T, et al. (2005) A duplicated pair of *Arabidopsis* RING-finger E3 ligases contribute to the RPM1- and RPS2-mediated hypersensitive response. *Plant J* 44:258–270.
22. Wandinger SK, Richter K, Buchner J (2008) The Hsp90 chaperone machinery. *J Biol Chem* 283:18473–18477.
23. Stitt M, Lilley RM, Heldt HW (1982) Adenine nucleotide levels in the cytosol, chloroplasts, and mitochondria of wheat leaf protoplasts. *Plant Physiol* 70:971–977.
24. Prodromou C, et al. (2000) The ATPase cycle of Hsp90 drives a molecular ''clamp'' via transient dimerization of the N-terminal domains. *EMBO J* 19:4383–4392.
25. Chen S, Sullivan WP, Toft DO, Smith DF (1998) Differential interactions of p23 and the TPR-containing proteins Hop, Cyp40, FKBP52, and FKBP51 with Hsp90 mutants. *Cell Stress Chaperones* 3:118–129.
26. Obermann WM, Sondermann H, Russo AA, Pavletich NP, Hartl FU (1998) In vivo function of Hsp90 is dependent on ATP binding and ATP hydrolysis. *J Cell Biol* 143:901–910.
27. Panaretou B, et al. (1998) ATP binding and hydrolysis are essential to the function of the Hsp90 molecular chaperone in vivo. *EMBO J* 17:4829–4836.
28. Ali MM, et al. (2006) Crystal structure of an Hsp90-nucleotide-p23/Sba1 closed chaperone complex. *Nature* 440:1013–1017.
29. Mickler M, Hessling M, Ratzke C, Buchner J, Hugel T (2009) The large conformational changes of Hsp90 are only weakly coupled to ATP hydrolysis. *Nat Struct Mol Biol* 16:281–286.
30. Hessling M, Richter K, Buchner J (2009) Dissection of the ATP-induced conformational cycle of the molecular chaperone Hsp90. *Nat Struct Mol Biol* 16:287–293.
31. Grant MR, et al. (1995) Structure of the *Arabidopsis RPM1* gene enabling dual specificity disease resistance. *Science* 269:843–846.
32. Mindrinos M, Katagiri F, Yu G-L, Ausubel FM (1994) The *A. thaliana* disease resistance gene *RPS2* encodes a protein containing a nucleotide-binding site and leucine-rich repeats. *Cell* 78:1089–1099.
33. Ritter C, Dangl JL (1996) Interference between 2 specific pathogen recognition events mediated by distinct plant disease resistance genes. *Plant Cell* 8:251–257.
34. Holt BF III, et al. (2002) An evolutionarily conserved mediator of plant disease resistance gene function is required for normal *Arabidopsis* development. *Dev Cell* 2:807–817.
35. Koch E, Slusarenko AJ (1990) *Arabidopsis* is susceptible to infection by a downy mildew fungus. *Plant Cell* 2:437–445.
36. Serebriiskii IG, Toby GG, Golemis EA (2000) Streamlined yeast colorimetric reporter activity assays using scanners and plate readers. *BioTechniques* 29:278–279, 282–284, 286–288.
37. Richter K, Muschler P, Hainzl O, Buchner J (2001) Coordinated ATP hydrolysis by the Hsp90 dimer. *J Biol Chem* 276:33689–33696.

Supporting Information

Hubert et al. 10.1073/pnas.0904877106

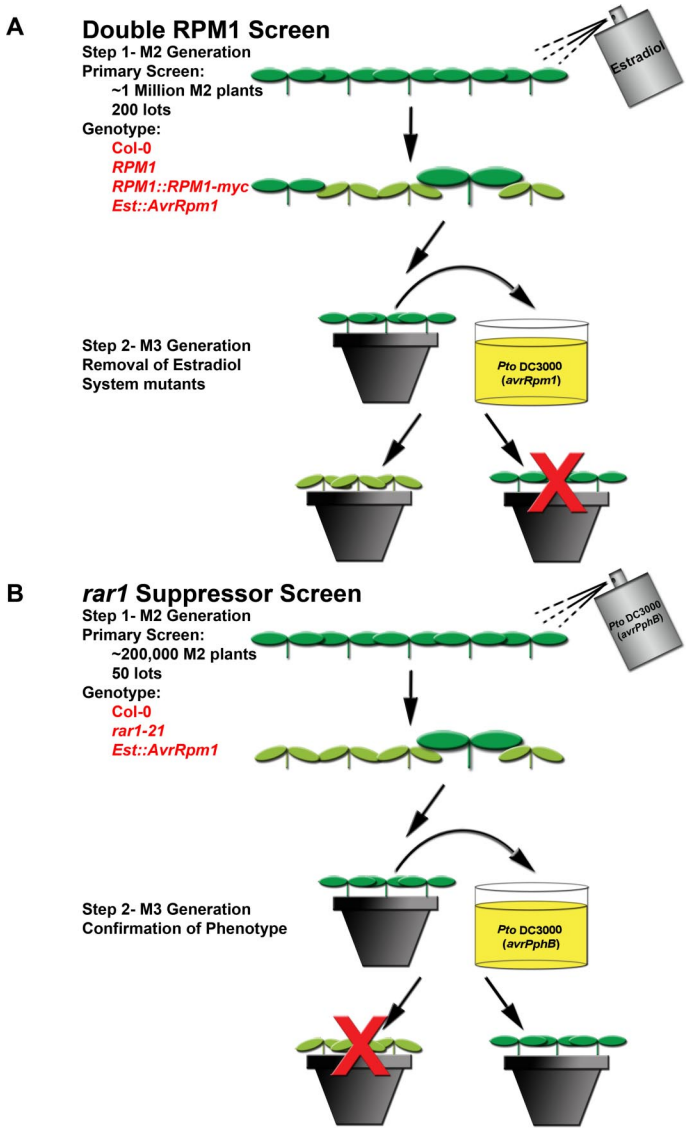

Fig. S1. Two genetic screens to identify genes involved in plant disease resistance. These flow charts depict the process conducted in both genetic screens. (*A*) The Double RPM1 Screen began with wild-type Columbia-0 plants expressing *RPM1*. An estradiol-inducible version of the bacterial gene *AvrRpm1* was introduced along with an *RPM1* transgene carrying a myc-epitope-tagged version of RPM1 under the control of its native promoter (1, 2). This line was mutagenized, and ≈100 M_1 plants were allowed to self in each of 200 separate pools or lots. *AvrRpm1* expression in the resulting M_2 plants was induced with estradiol. Seed was collected from nonresponsive plants. These M_3 plants were then tested for resistance to *Pto* DC3000(*avrRpm1*). This step allowed the identification and removal of plants with mutations in the estradiol-inducible expression system. (*B*) The *rar1* suppressor screen was begun by mutagenizing *rar1–21* mutant seed (2) carrying the same estradiol-inducible version of *AvrRpm1* as in *A*. The resulting M_1 plants were allowed to self in 50 separate lots. M_2 plants were sprayed with *Pto* DC3000(*avrPphB*). Disease-resistant plants were allowed to self, and resulting M_3 plants were retested by dip inoculation in separately in both *Pto* DC3000(*avrPphB*) and (*avrRpm1*) to confirm the disease-resistant phenotype.

1. Boyes DC, Nam J, Dangl JL (1998) The *Arabidopsis thaliana RPM1* disease resistance gene product is a peripheral plasma membrane protein that is degraded coincident with the hypersensitive response. *Proc Natl Acad Sci USA* 95:15849–15854.
2. Tornero P, et al. (2002) *RAR1* and *NDR1* contribute quantitatively to disease resistance in *Arabidopsis* and their relative contributions are dependent on the *R* gene assayed. *Plant Cell* 14:1005–1015.

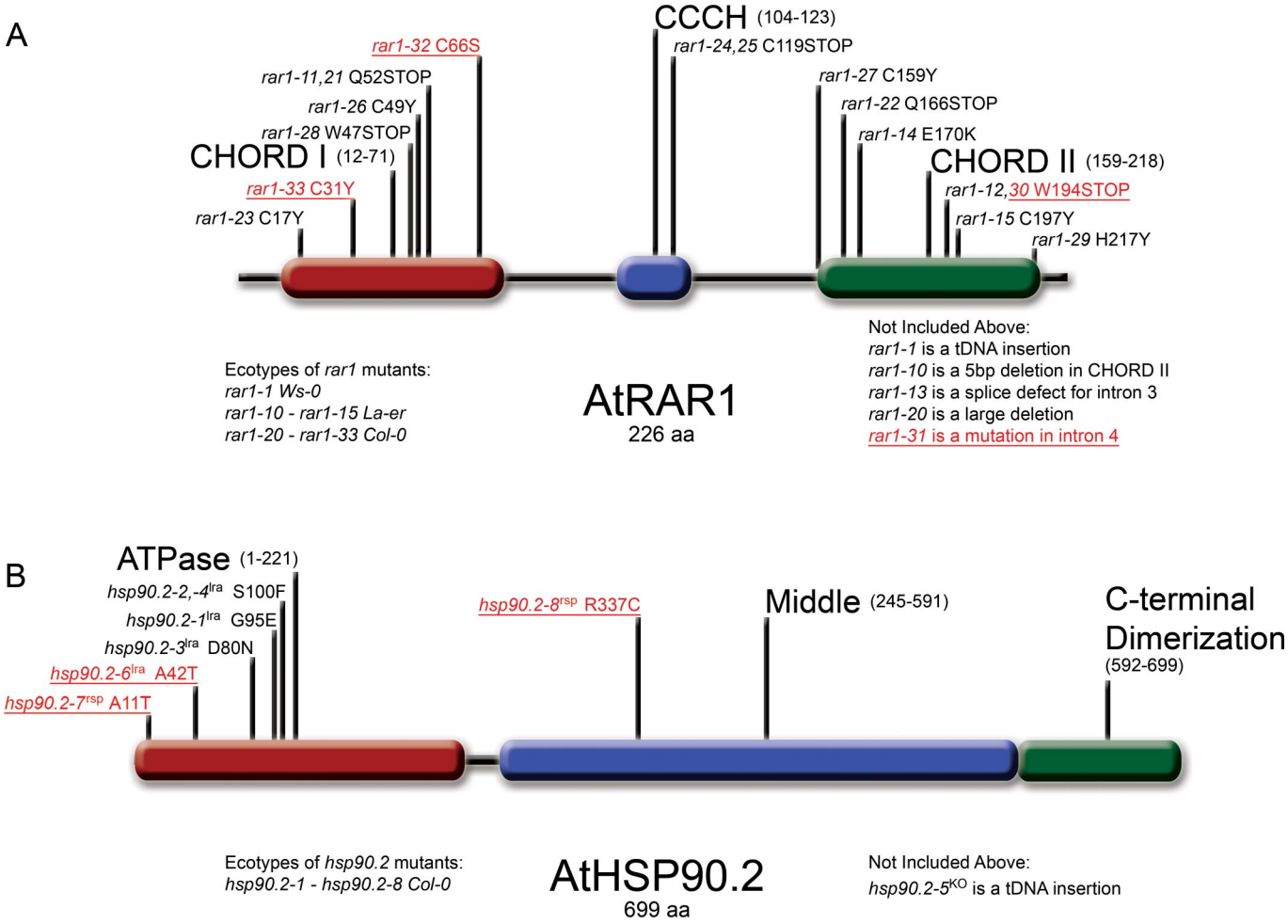

Fig. S2. Schematic representations of *Arabidopsis* RAR1 and HSP90.2 showing the location of all known mutant alleles. Alleles introduced in this article are underlined and in red. (*A*) Identified mutations in RAR1. The CHORD-I domain is shown in red, the CCCH region is shown in blue, and the CHORD-II domain is shown in green. The allele designation and associated amino acid change are shown in relation to its linear position. The ecotypes in which the mutants were identified are shown below. Noncoding mutations are described below the linear molecule. (*B*) Identified mutations in HSP90.2. The ATPase domain is shown in red, the middle domain is shown in blue, and the C-terminal dimerization domain is shown in green. The phenotype of the respective mutation is indicated after the allele designation and associated amino acid change, *lra* for loss of recognition of avrRpm1 and *rsp* for rar1 suppressor.

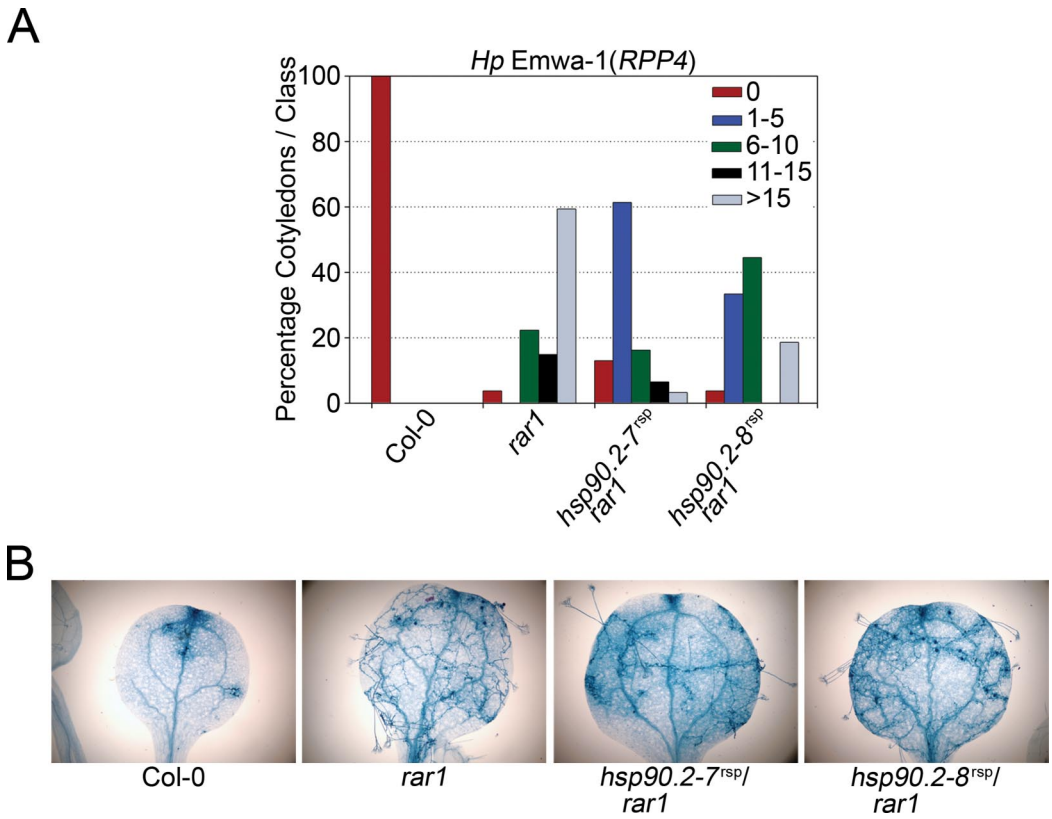

Fig. S3. *hsp90.2*^{rsp} alleles suppress the *rar1* effect on *RPP4*, a TIR-NB-LRR, in response to an oomycete pathogen, *Hpa*, isolate Emwa1. (*A*) The *RAR1*-dependent TIR-NB-LRR protein RPP4 conditions recognition of the *Hpa* isolate Emwa-1 in wild-type Col-0 plants. Consequently, there is no oomycete sporulation in these plants. RAR1 is required for RPP4-mediated recognition. Consequently, *rar1* mutants display a high level of *Hpa* reproduction. *hsp90.2*^{rsp} *rar1* double mutants both display more sporangiophores than wild-type plants but less than a *rar1* single mutant, suggesting partial suppression of *rar1* for RPP4 function. Colored bars refer to the number of sporangiophores counted per cotyledon. Minimum of 20 cotyledons per genotype was used. (*B*) Trypan blue staining of dead plant cells and oomycete hyphal structures is shown. Dead xylem cells in the vascular bundle can be seen in all genotypes. While areas of death representing a HR can be seen in Col-0, fine hair-like hyphae can be seen in, and reproductive sporangiophores are shown radiating from, the *rar1* cotyledon. The *hsp90.2*^{rsp} *rar1* double mutants support intermediate levels of *Hpa* growth and the trailing necrosis associated with partial NB-LRR function.

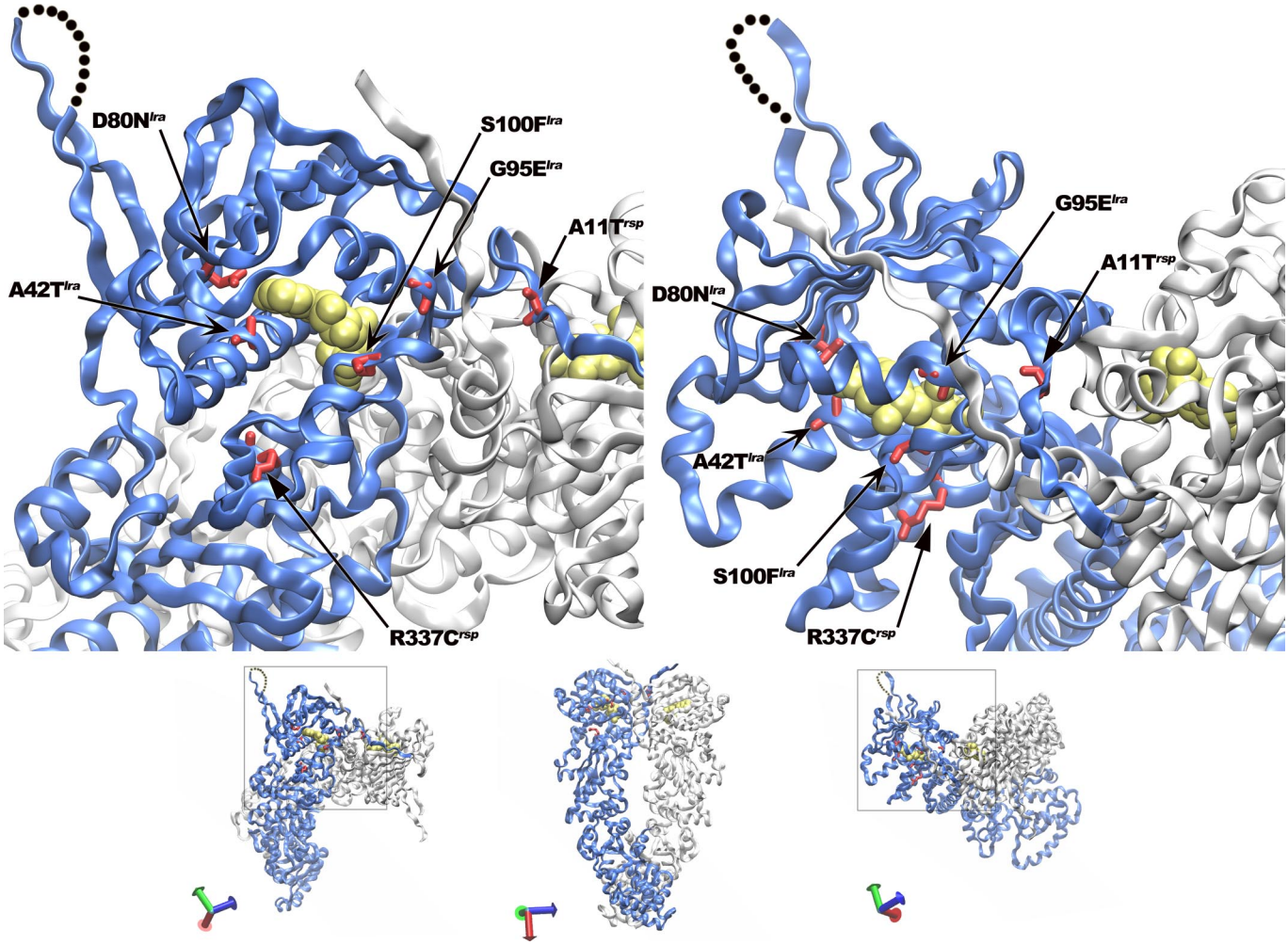

Fig. S4. All identified *AtHSP90.2* mutations in *Arabidopsis* lie within or near the ATPase domain. Ribbon structure close-up of the crystal structure of the yeast HSP90 dimer (Protein Data Bank ID code 2CG9) showing the locations of the residues mutated in AtHSP90.2 in red. Individual HSP90 monomers are shown in light gray and blue. The lra or rsp designation of each respective mutant is shown after the residue. ATP is shown in pale yellow. A view of the full dimer is shown underneath with the area of the close-up represented in a box. Axes are shown for orientation. Residue numbering relates to position in AtHSP90.2, inferred by alignment with yeast HSP90.

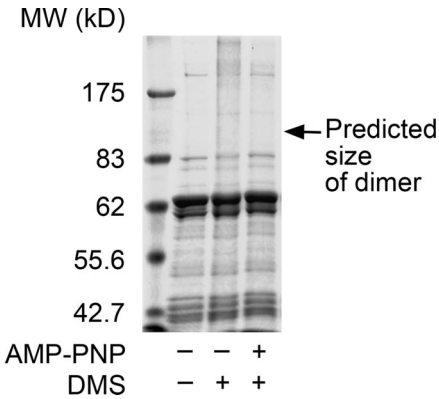

Fig. S5. The AtHSP90.2 ATPase domain is insufficient for dimer formation. A C-terminal truncation of HSP90 is unable to dimerize in a chemical cross-linking experiment. The protein was tested without nucleotide or with 10 mM of the nonhydrolysable ATP analog, AMP-PNP. The experiment shown was conducted at 0.25 mg/mL of HSP90 ΔC and 15 molar equivalents of DMS; similar results were obtained with 30 molar equivalents and the cross-linkers DSS and DMP.

Table S1. Previously-identified HSP90 mutations

Mutation position in reference to AtHSP90.2	Mutation position in reference to ScHSP90	Mutation position in original organism	Species	Mutant name	Protein	Phenotype	Source/ref.
Single amino acid changes							
E5R	E4R	E6R	*Triticum aestivum*		TaHSP90	Reduced binding to the CS domain of SGT1 and AtRAR1	1
A11T	A10T	A11T	*Arabidopsis thaliana*	A*thsp90.2–7*	AtHSP90.2	Restoration of NB-LRR function and accumulation in a rar1 mutant; normal ATPase activity; normal dimerization; normal RAR1 interaction; decreased SGT1 interaction	This study
T23I	T22I	T22I	*Saccharomyces cerevisiae*		ScHSP82	Impairs AhR signaling; temperature sensitivity; reduced GR activity; osmosensitive; increased ATPase activity; reduced interaction with cdc37; reduced accumulation of GR; enhanced AMP-PNP binding; enhanced N-terminal dimerization	2–7
T23I	T22I	T22I	*Saccharomyces cerevisiae*		ScHSC82	Temperature sensitive growth defect; reduced GR and v-Src activities; enhanced ATPase activity; reduced GR accumulation; reduced interactions with client protein Sti1 and Sba1	8
T23F	T22F	T22F	*Saccharomyces cerevisiae*		ScHSC82	Increases ATP hydrolysis	9
F24A	V23A	V23A	*Saccharomyces cerevisiae*		ScHSC82	4.8-fold reduction of ATP hydrolysis (compared with WT)	9
Y25A	Y24A	Y24A	*Saccharomyces cerevisiae*		ScHSC82	4.8-fold reduction of ATP hydrolysis	9
E292K	E301K	E292K	*Caenorhabditis elegans*	*daf-21(p673)*	CeHSP90	Defects in specific chemosensory responses; reduced fertility	10
E34A	E33A	E33A	*Saccharomyces cerevisiae*		ScHSP82	Decreased ATP hydrolysis	11, 12
E34A	E33A	E33A	*Saccharomyces cerevisiae*		ScHSC82	Abolishes ATP hydrolysis	9
E34A	E33A	E46A	*Gallus gallus*		HSP90α	Loses the ability to assist HSP70, HSP40 and HOP in the refolding protein; abolishes ATP hydrolysis	13
S36L	S37L	S38L	*Drosophila melanogaster*	*E(sev)3A e1D*	HSP83	Lethality; reduced Raf kinase activity; reduced binding to Raf	14, 15
N38A	N37A	N50A	*Gallus gallus*		HSP90α	Abolishes nucleotide binding and interacting with p23	13
A42V	A41V	A41V	*Saccharomyces cerevisiae*		ScHSP82	Impairs AhR signaling; temperature sensitivity; reduced GR activity; reduced accumulation of GR; enhanced AMP-PNP binding; reduced ATPase acitivity	3, 4, 6
A42T	A41T	A42T	*Arabidopsis thaliana*	A*thsp90.2–6*	AtHSP90.2	Loss of RPM1 function and accumulation; fully penetrant phenotype; loss of ATPase activity; loss of dimerization; loss of RAR1 interaction; loss of SGT1 interaction	This study
R47C	R46C	R48C	*Drosophila melanogaster*	*13F3*	HSP83	Reduced Raf kinase activity	15
D80N	D79N	D79N	*Saccharomyces cerevisiae*		ScHSP82	Growth retardation; decreased binding to ATP, ADP and p23	11, 12
D80N	D79N	D79N	*Saccharomyces cerevisiae*		ScHSC82	Reduced interactions with client protein Sba1 and Cpr6	8
D80N	D79N	D92A	*Gallus gallus*		HSP90α	Abolishes nucleotide binding and interacting with p23	13
D80N	D79N	D80N	*Arabidopsis thaliana*	A*thsp90.2–3*	AtHSP90.2	Loss of RPM1 function and accumulation; fully penetrant phenotype; loss of ATPase activity; loss of dimerization; loss of RAR1 interaction; loss of SGT1 interaction	16; this study
G82S	G81S	G81S	*Saccharomyces cerevisiae*		ScHSP82	Impairs AhR signaling; temperature sensitivity; reduced GR activity; osmosensitive	3, 4, 7

Mutation position in reference to AtHSP90.2	Mutation position in reference to ScHSP90	Mutation position in original organism	Species	Mutant name	Protein	Phenotype	Source/ref.
G84C	G83C	G84C	*Schizosaccharomyces pombe*	*swo1–25 (swo1–26)*	SpHSP90	Temperature sensitivity; impaired glucose repression of fbp1(+) transcription; suppresses cell cycle arrest caused by overexpression of wee1 (+); advances mitosis; reduces the stability of the client protein Wee1	17, 18
T86E	T85E	T87E	*Triticum aestivum*		TaHSP90	Reduced binding to the CS domain of SGT1	1
K87E	K86E	K86E	*Saccharomyces cerevisiae*		ScHSP82	Reduced binding to the CS domain of SGT1	1
K87E	K86E	K88E	*Triticum aestivum*		TaHSP90	Reduced binding to the CS domain of SGT1; genetically suppresses AtSGT1a E223K mutant	1
A88E	A87E	S89E	*Triticum aestivum*		TaHSP90	Reduced binding to AtSGT1a	19
D89R	E88R	D90R	*Triticum aestivum*		TaHSP90	Reduced binding to the CS domain of SGT1 and AtRAR1	1
V91T	I90T	V92T	*Triticum aestivum*		TaHSP90	Reduced binding to AtSGT1a	19
N92R	N91R	N93R	*Triticum aestivum*		TaHSP90	Reduced binding to the CS domain of SGT1	1
G95E	G94E	G95E	*Arabidopsis thaliana*	*Athsp90.2–1*	AtHSP90.2	Loss of RPM1 function and accumulation; fully penetrant phenotype; loss of ATPase activity; loss of dimerization; loss of RAR1 interaction; loss of SGT1 interaction	16, This study
A98I	A97I	A97I	*Saccharomyces cerevisiae*		ScHSP82	Reduced levels of hormone binding by the ER	20
A98T	A97T	A97T	*Saccharomyces cerevisiae*		ScHSP82	Temperature sensitive	21
R99A	K98A	K106A	*Homo sapiens*		hHSP90 α	Reduced binding to GA	22
R99E	K98E	R100E	*Triticum aestivum*		TaHSP90	Enhanced binding to the CS domain of SGT1	1
S100A	S99A	S113A	*Homo sapiens*		hHSP90 α	Abolishes binding to geldanamycin (GA) and ATP	23
S100F	S99F	S100F	*Arabidopsis thaliana*	*Athsp90.2–2, -4*	AtHSP90.2	Loss of RPM1 function and accumulation; partially penetrant phenotype; loss of ATPase activity; loss of dimerization; normal RAR1 interaction; loss of SGT1 interaction	16, this study
G101D	G100D	G113D	*Gallus gallus*		HSP90α	Does not bind to novobiocin	24
T102I	T101I	T101I	*Saccharomyces cerevisiae*		ScHSP82	Temperature sensitivity; decreases the growth rates on media containing 0.05% maltose; reduced maltose induction; shortens the half-life of the client protein Mal63p which is a MAL activator; reduced levels of hormone binding by the estrogen receptor (ER); reduced activity of substrate Hap1; reduced GR activity; reduced formation of CBF3-centromere DNA; hypersensitive to GA and RA; enhanced interaction with cdc37; reduced nucleotide binding; reduced ATPase acitivity; diminished N-terminal dimerization	2, 4–7, 20, 21, 25–28
T102I	T101I	T101I	*Saccharomyces cerevisiae*		ScHSC82	Temperature sensitive growth defect; reduced GR and v-Src activities; reduced ATPase activity; reduced v-Scr accumulation; reduced interactions with Sba1 and Cpr6	8
A108N	A107N	A107N	*Saccharomyces cerevisiae*		ScHSC82	Reduced interaction with Sti1	8
A132D	A131D	A133D	*Drosophila melanogaster*		HSP83	Affected localization of nanos and pgc mRNA	29

Mutation position in reference to AtHSP90.2	Mutation position in reference to ScHSP90	Mutation position in original organism	Species	Mutant name	Protein	Phenotype	Source/ref.
D144R	D143R	D143R	*Saccharomyces cerevisiae*		ScHSP82	Reduced binding to the CS domain of SGT1	1
D144R	D143R	D145R	*Triticum aestivum*		TaHSP90	Reduced binding to the CS domain of SGT1 and AtRAR1	1
E145R	E144R	E146R	*Triticum aestivum*		TaHSP90	Reduced binding to the CS domain of SGT1	1
G155D	G154D	G155D	*Schizosaccharomyces pombe*	*swo1-w1*	SpHSP90	Sensitive to stressful growth conditions; mitotic defects	17, 18
G171D	G170D	G170D	*Saccharomyces cerevisiae*		ScHSP82	Temperature sensitivity; abolishes the activity of protein kinase Gcn2; increases HSF-dependent gene expression; abolishes the high affinity ligand binding conformation of human androgen receptor (AR); reduced levels of hormone binding by the ER; decreased activity of $p60^{V\text{-}src}$; reduced GR activity at high temperature; declines in telomere length; loses p23 binding and ATPase activity; abolishes the accumulation of Gcn2; reduced telomerase DNA binding	3, 4, 6, 20, 21, 27, 30–33
K265A	K274A	K294A	*Homo sapiens*		hHSP90 α	Mimic acetylated; reduced binding to cochaperon p23 and client protein ErbB2	34
K265Q	K274Q	K294Q	*Homo sapiens*		hHSP90 α	Mimic acetylated; reduced binding to Cochaperone p23 and client protein ErbB2	34
K265R	K274R	K294R	*Homo sapiens*		hHSP90 α	Unacetylated	34
W268G	W277G	W297G	*Homo sapiens*		hHSP90 α	Blocks self-oligomerization	35
W291A	W300A	W296A	*Saccharomyces cerevisiae*		ScHSC82	Reduced interaction with Sti1	8
W291A	W300A	W300A	*Saccharomyces cerevisiae*		ScHSP82	Temperature sensitive growth defect; reduced GR activity; enhanced v-Scr activity; reduced binding to Aha1; increased v-Scr accumulation	(2
E303K	E312K	E317K	*Drosophila melanogaster*	*Esev)3A e6D*	HSP83	Lethality; reduced Raf kinase activity; affected localization of nanos and pgc mRNA; reduced binding to Raf	14, 15, 29
G304N	G313N	G313N	*Saccharomyces cerevisiae*		ScHSP82	Affects all receptor types tested; temperature sensitivity; decreased growth rates; constitutive expression of transcription factor Gcn4; reduced levels of hormone binding by the ER; reduced activity of substrate Hap1; defective pheromone-signaling; decreases GR ligand binding activity; unstable aporeceptor complexes; reduced accumulation of substrate proteins Ste7 and Ste11	22, 28, 32, 36, 37
G304N	G313N	G329N	*Gallus gallus*		HSP90α	Affects interacting with HSP90 accessory proteins	38
G304S	G313S	G313S	*Saccharomyces cerevisiae*		ScHSP82	Impairs AhR signaling; reduced activity of substrate Hap1 and GR; temperature sensitivity	3, 4, 26
F320A	F329A	F325A	*Saccharomyces cerevisiae*		ScHSC82	Reduced interaction with Sti1	8
L334P	L343P	L338P	*Schizosaccharomyces pombe*	*git10–201*	SpHSP90	CAMP signaling defect; impaired glucose repression of fbp1(+) transcription	17
R337C	R346C	R337C	*Arabidopsis thaliana*	A*thsp90.2–8*	AtHSP90.2	Restoration of NB-LRR function and accumulation in a rar1 mutant; loss of ATPase activity; decreased dimerization; loss of RAR1 interaction; loss of SGT1 interaction	This study

Mutation position in reference to AtHSP90.2	Mutation position in reference to ScHSP90	Mutation position in original organism	Species	Mutant name	Protein	Phenotype	Source/ref.
F340A	F349A	F345A	*Saccharomyces cerevisiae*		ScHSC82	Reduced interaction with Sba1 and Cpr6	8
P350A	P359A	P379A	*Homo sapiens*		hHSP90 α	Blocks self-oligomerization	35
F355A	F364A	F384A	*Homo sapiens*		hHSP90 α	Blocks self-oligomerization	35
E363K	E372K	E377K	*Drosophila melanogaster*	*9J1*	HSP83	Reduced Raf kinase activity	15
L367D	L376D	L372D	*Saccharomyces cerevisiae*		ScHSC82	60-fold reduction of ATP hydrolysis	9
L367S	L376S	L392S	*Gallus gallus*		HSP90α	Reduced binding activity to p23	39
I369N	L378N	L374N	*Saccharomyces cerevisiae*		ScHSC82	3-fold reduction of ATP hydrolysis	9
R371A	R380A	R376A	*Saccharomyces cerevisiae*		ScHSC82	Reduced interaction with Sba1; 6.7 fold reduction of ATP hydrolysis	8, 9
E372K	E381K	E381K	*Saccharomyces cerevisiae*		ScHSP82	Impairs AhR signaling; temperature sensitivity; reduced GR activity; temperature sensitive growth defect; reduced GR and v-Src activities; reduced GR and v-Scr accumulations	2–4
E372K	E381K	E377K	*Saccharomyces cerevisiae*		ScHSC82	Reduced interaction with Sti1	8
E422K	E431K	E431K	*Saccharomyces cerevisiae*		ScHSP82	Affects glucocorticoid receptor (GR) signaling; Impairs Aryl hydrocarbon receptor (AhR) signaling; reduced levels of hormone binding by the ER; temperature sensitive growth defect; reduced v-Src activity; reduced ATPase activity; reduced GR accumulation	2, 3, 20, 36, 37
L448A	L457A	L477A	*Homo sapiens*		hHSP90 α	Blocks self-oligomerization; blocks binding to HtpGA	40
S476K	S485K	S485K	*Saccharomyces cerevisiae*		ScHSP82	Reduced levels of hormone binding by the ER	20
S476Y	S485Y	S485Y	*Saccharomyces cerevisiae*		ScHSP82	Temperature-sensitive growth defect; reduced GR and v-Src activities; reduced ATPase activity; reduced binding to p23 and AhaI; reduced v-Scr accumulation	2, 21
S476Y	S485Y	S481Y	*Saccharomyces cerevisiae*		ScHSC82	Reduced interactions with Sba1 and Cpr6	8
L482S	L491S	L487S	*Saccharomyces cerevisiae*		ScHSC82	Reduced interactions with Sba1 and Cpr6	8
E488A	E497E	E517A	*Homo sapiens*		hHSP90 α	Blocks self-oligomerization; blocks binding to HtpGA	40
ΔY491	ΔF500	ΔF492	*Podospora anserina*	*mod-E1*	Member of HSP90 family	Alters the sexual cycle and partially suppresses vegetative incompatibility	41
T516I	T525I	T525I	*Saccharomyces cerevisiae*		ScHSP82	Affects all receptor types tested; temperature sensitivity; decreased growth rates; constitutive expression of transcription factor Gcn4; decreases GR ligand binding activity; unstable aporeceptor complexes; reduced GR and v-Src activities; reduced ATPase activity; reduced binding to p23 and AhaI; reduced v-Scr accumulation	2, 21, 30, 36, 37
T516I	T525I	T521I	*Saccharomyces cerevisiae*		ScHSC82	Reduced interactions with Sba1 and Cpr6	8
T516I	T525I	T541I	*Gallus gallus*		HSP90α	Affects interacting with HSP90 accessory proteins	38
K532Q	R540Q	M553Q	*Homo sapiens*		hHSP90β	Moderately enhances dimeric activity	42
E537A	K545A	T566A	*Homo sapiens*		hHSP90 α	Decreased dimeric activity	42
E537T	K545T	A558T	*Homo sapiens*		hHSP90β	Enhances dimeric activity	42
E537V	K545V	A558V	*Homo sapiens*		hHSP90β	Enhances dimeric activity	42
E537I	K545I	A558I	*Homo sapiens*		hHSP90β	Enhances dimeric activity	42
E537R	K545R	A558R	*Homo sapiens*		hHSP90β	Enhances dimeric activity	42
E537Y	K545Y	A558Y	*Homo sapiens*		hHSP90β	Moderately enhances dimeric activity	42
S560C	S568C	S574C	*Drosophila melanogaster*	*E(sev)3A e3A*	HSP83	Lethality	14
D565T	D537T	S586T	*Homo sapiens*		hHSP90β	Moderately enhances dimeric activity	42
T578F	S586F	S592F	*Drosophila melanogaster*	*E(sev)3A e6A*	HSP83	Lethality; affected localization of nanos and pgc mRNA	14, 29

Mutation position in reference to AtHSP90.2	Mutation position in reference to ScHSP90	Mutation position in original organism	Species	Mutant name	Protein	Phenotype	Source/ref.
A579T	A587T	A587T	*Saccharomyces cerevisiae*		ScHSP82	Temperature sensitivity; reduced GR activity; hypersensitive to GA and RD; reduced activity of substrate Hap1	4, 7, 26
A579T	A587T	A583T	*Saccharomyces cerevisiae*		ScHSC82	Reduced interactions with Sba1 and Cpr6	8
S600A	S608M	A629M	*Homo sapiens*		hHSP90 α	Decreased dimeric activity	42
S600A	S608A	M621A	*Homo sapiens*		hHSP90β	Enhances dimeric activity	42
S600W	S608W	M621W	*Homo sapiens*		hHSP90β	Moderately enhances dimeric activity	42
S600V	S608V	M621V	*Homo sapiens*		hHSP90β	Moderately enhances dimeric activity	42
D615A	K623A	E644A	*Homo sapiens*		hHSP90 α	Increased chaperon activity	43
D622A	D630A	E651A	*Homo sapiens*		hHSP90 α	Decreased chaperon activity; inhibited binding to Hop	43
D624A	G632A	D653A	*Homo sapiens*		hHSP90 α	Decreased chaperon activity; abolished binding to Hop	43
L635I	K644I	V656I	*Homo sapiens*		hHSP90β	Enhances dimeric activity	42
E639A	E648A	E668A	*Homo sapiens*		hHSP90 α	Increased chaperon activity	43
A641F	A650F	S655F	*Drosophila melanogaster*	*E(sev3A e4A*	HSP83	Lethality	14
L649R	L658R	L654R	*Schizosaccharomyces pombe*	*swo1–21*	SpHSP90	Temperature- sensitive growth defect; impaired glucose repression of fbp1(+) transcription	17
F655A	F664A	F660A	*Saccharomyces cerevisiae*		ScHSC82	Reduced interactions with Sba1 and Cpr6	8
E685A	E698A	E720A	*Homo sapiens*		hHSP90 α	Abolished binding to PP5 and FKBP52	43
D687A	P700A	D722A	*Homo sapiens*		hHSP90 α	Abolished binding to PP5 and FKBP52	43
A688A	A701A	D723A	*Homo sapiens*		hHSP90 α	Abolished binding to PP5 and FKBP52	43
D689A	D702A	D724A	*Homo sapiens*		hHSP90 α	Abolished binding to PP5 and FKBP52	43
E696A	E706A	E729A	*Homo sapiens*		hHSP90 α	Abolished binding to TPR proteins	43
E697A	E707A	E730A	*Homo sapiens*		hHSP90 α	Abolished binding to TPR proteins	43
D699A	D709A	D732A	*Homo sapiens*		hHSP90 α	Abolished binding to TPR proteins	43
Changes involving 2 or more amino acids							
T23F/R371A	T22F/R380A	T22F/R376A	*Saccharomyces cerevisiae*		ScHSC82	1.6-fold reduction of ATP hydrolysis	9
F24A/R371A	V23A/R380A	V23A/R376A	*Saccharomyces cerevisiae*		ScHSC82	20-fold reduction of ATP hydrolysis	9
Y25A/R371A	Y24A/R380A	Y24A/R376A	*Saccharomyces cerevisiae*		ScHSC82	24-fold reduction of ATP hydrolysis	9
S219A/E239A	P218A/E249A	S226A/S255A	*Homo sapiens*		hHSP90β	Increased transcription activity of AhR gene; phosphorylation defect; enhanced interaction with AhR; reduces the resistance of mouse cell to cytochrome c; inhibits phosphorylation; enhances binding to client protein Apaf-1	44, 45
F320A/L322A/F323A	F329A/L331A/F332A	F329A/L331A/F332A	*Saccharomyces cerevisiae*		ScHSP82	Reduced GR and v-Src activities	2
R337A/R338A	R346A/R347A	R362A/R363A	*Gallus gallus*		HSP90α	Abolishes binding to p23	39
L369N/R371A	L378N/R380A	L374N/R376A	*Saccharomyces cerevisiae*		ScHSC82	24-fold reduction of ATP hydrolysis	9
A568T/V571K	A576T/R579K	A576T/R579K	*Saccharomyces cerevisiae*		ScHSP82	Affects all receptor types tested; temperature sensitivity; decreased growth rates; decreases GR ligand binding activity; unstable aporeceptor complexes	36, 37
I584A/M585A	I592A/M593A	I588A/M589A	*Saccharomyces cerevisiae*		ScHSC82	Reduced interactions with Sba1 and Cpr6	8
L636S/L637S	L645S/L646S	L665S/L666S	*Homo sapiens*		hHSP90 α	Blocks self-oligomerization and binding to client protein	46
L642S/L643S	L651S/L652S	L647S/L648S	*Saccharomyces cerevisiae*		ScHSC82	Reduced interactions with Sba1 and Cpr6	8
L642S/L643S	L651S/L652S	L671S/L672S	*Homo sapiens*		hHSP90 α	Blocks self-oligomerization and binding to client protein	46
E696A/E697A	E706A/E707A	E725A/E726A	*Gallus gallus*		HSP90α	Affects interacting with HSP90 accessory proteins	38

Neither the *rsp* phenotype nor the *rsp* allele mutations have been previously observed. This is a comprehensive list of previously-identified HSP90 mutations identified from all organisms in relation to HSP90.2 amino acid sequence. Mutations are given in relation to *At*HSP90.2 and *Sc*HSP82 sequence and the sequence of the originally-identified mutation. Genetic and biochemical characterization of each mutation is also given. Truncations and large deletions have been omitted.

1. Boyes DC, Nam J, Dangl JL (1998) The *Arabidopsis thaliana RPM1* disease resistance gene product is a peripheral plasma membrane protein that is degraded coincident with the hypersensitive response. *Proc Natl Acad Sci USA* 95:15849–15854.
2. Tornero P, et al. (2002) *RAR1* and *NDR1* contribute quantitatively to disease resistance in *Arabidopsis* and their relative contributions are dependent on the *R* gene assayed. *Plant Cell* 14:1005–1015.
3. Kadota Y, et al. (2008) Structural and functional analysis of SGT1-HSP90 core complex required for innate immunity in plants. *EMBO Rep* 9:1209–1215.
4. Hawle P, et al. (2006) The middle domain of Hsp90 acts as a discriminator between different types of client proteins. *Mol Cell Biol* 26:8385–8395.
5. Cox MB, Miller CA, 3rd (2004) Cooperation of heat shock protein 90 and p23 in aryl hydrocarbon receptor signaling. *Cell Stress Chaperones* 9:4–20.
6. Nathan DF, Lindquist S (1995) Mutational analysis of Hsp90 function: Interactions with a steroid receptor and a protein kinase. *Mol Cell Biol* 15:3917–3925.
7. Millson SH, et al. (2004) Investigating the protein–protein interactions of the yeast Hsp90 chaperone system by two-hybrid analysis: Potential uses and limitations of this approach. *Cell Stress Chaperones* 9:359–68.
8. Prodromou C, et al. (2000) The ATPase cycle of Hsp90 drives a molecular &lquote;clamp' via transient dimerization of the N-terminal domains. *EMBO J* 19:4383–4392.
9. Peter W, et al. (2003) Sensitivity to Hsp90-targeting drugs can arise with mutation to the Hsp90 chaperone, cochaperones and plasma membrane ATP binding cassette transporters of yeast. *Eur J Biochem* 270:4689–4695.
10. Johnson JL, Halas A, Flom G (2007) Nucleotide-dependent interaction of *Saccharomyces cerevisiae* Hsp90 with the cochaperone proteins Sti1, Cpr6, and Sba1. *Mol Cell Biol* 27:768–776.
11. Cunningham CN, Krukenberg KA, Agard DA (2008) Intra- and intermonomer interactions are required to synergistically facilitate ATP hydrolysis in Hsp90. *J Biol Chem* 283:21170–21178.
12. Birnby DA, et al. (2000) A transmembrane guanylyl cyclase (DAF-11) and Hsp90 (DAF-21) regulate a common set of chemosensory behaviors in *Caenorhabditis elegans*. *Genetics* 155:85–104.
13. Obermann WMJ, Sondermann H, Russo AA, Pavletich NP, Hartl FU (1998) In vivo function of Hsp90 is dependent on ATP binding and ATP hydrolysis. *J Cell Biol* 143:901–910.
14. Panaretou B, et al. (1998) ATP binding and hydrolysis are essential to the function of the Hsp90 molecular chaperone in vivo. *EMBO J* 17:4829–4836.
15. Grenert JP, Johnson BD, Toft DO (1999) The importance of ATP binding and hydrolysis by Hsp90 in formation and function of protein heterocomplexes. *J Biol Chem* 274:17525–17533.
16. Cutforth T, Rubin GM (1994) Mutations in Hsp83 and cdc37 impair signaling by the sevenless receptor tyrosine kinase in *Drosophila*. *Cell* 77:1027–1036.
17. van der Straten A, Rommel C, Dickson B, Hafen E (1997) The heat shock protein 83 (Hsp83) is required for Raf-mediated signalling in *Drosophila*. *EMBO J* 16:1961–1969.
18. Hubert DA, et al. (2003) Cytosolic HSP90 associates with and modulates the *Arabidopsis* RPM1 disease resistance protein. *EMBO J* 22:5679–5689.
19. Alaamery MA, Hoffman CS (2008) *Schizosaccharomyces pombe* Hsp90/Git10 is required for glucose/cAMP signaling. *Genetics* 178:1927–1936.
20. Aligue R, Akhavan-Niak H, Russell P (1994) A role for Hsp90 in cell cycle control: Wee1 tyrosine kinase activity requires interaction with Hsp90. *EMBO J* 13:6099–6106.
21. Zhang M, et al. (2008) Structural and functional coupling of Hsp90- and Sgt1-centred multiprotein complexes. *EMBO J* 27:2789–2798.
22. Fliss AE, Benzeno S, Rao J, Caplan AJ (2000) Control of estrogen receptor ligand binding by Hsp90. *J Steroid Biochem Mol Biol* 72:223–230.
23. Kimura Y, Matsumoto S, Yahara I (1994) Temperature-sensitive mutants of hsp82 of the budding yeast *Saccharomyces cerevisiae*. *Mol Gen Genet* 242:517–527.
24. Onuoha SC, et al. (2007) Mechanistic studies on Hsp90 inhibition by ansamycin derivatives. *J Mol Biol* 372:287–297.
25. Lee Y-S, Marcu MG, Neckers L (2004) Quantum chemical calculations and mutational analysis suggest heat shock protein 90 catalyzes *trans-cis* Isomerization of geldanamycin. *Chem Biol* 11:991–998.
26. Marcu MG, Chadli A, Bouhouche I, Catelli M, Neckers LM (2000) The heat shock protein 90 antagonist novobiocin interacts with a previously unrecognized ATP-binding domain in the carboxyl terminus of the chaperone. *J Biol Chem* 275:37181–37186.
27. Bali M, Zhang B, Morano KA, Michels CA (2003) The Hsp90 molecular chaperone complex regulates maltose induction and stability of the *Saccharomyces* MAL gene transcription activator Mal63p. *J Biol Chem* 278:47441–47448.
28. Lee HC, Hon T, Zhang L (2002) The molecular chaperone Hsp90 mediates heme activation of the yeast transcriptional activator Hapl. *J Biol Chem* 277:7430–7437.
29. Toogun OA, DeZwaan DC, Freeman BC (2008) The Hsp90 molecular chaperone modulates multiple telomerase activities. *Mol Cell Biol* 28:457–467.
30. Stemmann O, Neidig A, Kocher T, Wilm M, Lechner J (2002) Hsp90 enables Ctf13p/Skp1p to nucleate the budding yeast kinetochore. *Proc Natl Acad Sci USA* 99:8585–8590.
31. Song Y, Fee L, Lee TH, Wharton RP (2007) The molecular chaperone Hsp90 is required for mRNA localization in *Drosophila melanogaster* embryos. *Genetics* 176:2213–2222.
32. Donze O, Picard D (1999) Hsp90 binds and regulates the ligand-inducible α -subunit of eukaryotic translation initiation factor kinase Gcn2. *Mol Cell Biol* 19:8422–8432.
33. Duina AA, Kalton HM, Gaber RF (1998) Requirement for Hsp90 and a CyP-40-type cyclophilin in negative regulation of the heat shock response. *J Biol Chem* 273:18974–18978.
34. Fang Y, Fliss AE, Robins DM, Caplan AJ (1996) Hsp90 regulates androgen receptor hormone binding affinity in vivo. *J Biol Chem* 271:28697–28702.
35. Nathan DF, Vos MH, Lindquist S (1997) In vivo functions of the *Saccharomyces cerevisiae* Hsp90 chaperone. *Proc Natl Acad Sci USA* 94:12949–12956.
36. Scroggins BT, et al. (2007) An acetylation site in the middle domain of Hsp90 regulates chaperone function. *Mol Cell* 25:151–159.
37. Nemoto TK, et al. (2004) The region adjacent to the highly immunogenic site and shielded by the middle domain is responsible for self-oligomerization/client binding of the HSP90 molecular chaperone. *Biochemistry* 43:7628–7636.
38. Bohen SP (1995) Hsp90 mutants disrupt glucocorticoid receptor ligand binding and destabilize aporeceptor complexes. *J Biol Chem* 270:29433–29438.
39. Bohen SP, Yamamoto KR (1993) Isolation of Hsp90 mutants by screening for decreased steroid receptor function. *Proc Natl Acad Sci USA* 90:11424–11428.
40. Chen S, Sullivan WP, Toft DO, Smith DF (1998) Differential interactions of p23 and the TPR-containing proteins Hop, Cyp40, FKBP52, and FKBP51 with Hsp90 mutants. *Cell Stress Chaperones* 3:118–129.
41. Chadli A, et al. (2000) Dimerization and N-terminal domain proximity underlie the function of the molecular chaperone heat shock protein 90. *Proc Natl Acad Sci USA* 97:12524–12529.
42. Matsumoto S, et al. (2002) Interaction between the N-terminal and middle regions is essential for the in vivo function of HSP90 molecular chaperone. *J Biol Chem* 277:34959–34966.
43. Loubradou G, Begueret J, Turcq B (1997) A mutation in an HSP90 gene affects the sexual cycle and suppresses vegetative incompatibility in the fungus *Podospora anserina*. *Genetics* 147:581–588.
44. Kobayakawa T, Yamada S, Mizuno A, Nemoto TK (2008) Substitution of only two residues of human Hsp90α causes impeded dimerization of Hsp90β. *Cell Stress Chaperones* 13:97–104.
45. Ramsey AJ, Russell LC, Whitt SR, Chinkers M (2000) Overlapping sites of tetratricopeptide repeat protein binding and chaperone activity in heat shock protein 90. *J Biol Chem* 275:17857–17862.
46. Ogiso H, et al. (2004) Phosphorylation analysis of 90-kDa heat shock protein within the cytosolic arylhydrocarbon receptor complex. *Biochemistry* 43:15510–15519.
47. Kurokawa M, Zhao C, Reya T, Kornbluth S (2008) Inhibition of apoptosome formation by suppression of Hsp90β phosphorylation in tyrosine kinase-induced leukemias. *Mol Cell Biol* 28:5494–506.
48. Yamada S, et al. (2003) A hydrophobic segment within the C-terminal domain is essential for both client-binding and dimer formation of the HSP90-family molecular chaperone. *Eur J Biochem* 270:146–154.